1,2,4,5-Tetrazine based ligands and complexes

Oleh Stetsiuk, Alexandre Abhervé, Narcis Avarvari

1,2,4,5-Tetrazine based ligands and complexes

Oleh Stetsiuk,[⊥] Alexandre Abhervé[⊥] and Narcis Avarvari*

MOLTECH-Anjou, UMR 6200, CNRS, UNIV Angers, 2 bd Lavoisier, 49045 ANGERS Cedex, France. E-mail: narcis.avarvari@univ-angers.fr

[⊥] These two authors have equally contributed to this work

Abstract

One of the most intriguing nitrogen based aromatic heterocycles is 1,2,4,5-tetrazine or *s*-tetrazine (TTZ) thanks to its electron acceptor character, fluorescent properties and possibilities of functionalization in the 3,6 positions allowing the access to various ligands. In this Review we focus on the two main families of TTZ based ligands, i.e. ditopic symmetric and monotopic non-symmetric, together with their metal complexes, with a special emphasis on the solid state structures and physical properties. After a description of the most representative complexes containing the unsubstituted TTZ as ligand, the symmetric TTZ ligands and complexes derived thereof are discussed in the order: 3,6-bis(2-pyridyl)-tetrazine, 3,6-bis(3-pyridyl)-tetrazine, 3,6-bis(4-pyridyl)-tetrazine, 3,6-bis(2-pyrimidyl)-tetrazine, 3,6-bis(2-pyrazinyl)-tetrazine, 3,6-bis(monopicolyamine)-tetrazine, 3,6-bis(vanillin-hydrazinyl)-tetrazine and TTZ containing carboxylic acids. Remarkable results have been obtained in the recent years in metal-organic frameworks and magnetic compounds in which the magnetic coupling is enhanced when the tetrazine bridge is reduced in radical anion. The non-symmetric ligands, such as dipicolylamine-TTZ and monopicolylamine-TTZ, are comparatively more recent than the symmetric ones. They allow in principle the preparation of mononuclear complexes in a controlled manner, although binuclear complexes have been isolated as well. Moreover, in the monopicolylamine-TTZ-Cl ligand, deprotonation of the amine, thanks to the electron acceptor character of TTZ, afforded a negatively charged ligand equivalent of a guanidinate.

1. Introduction

The chemistry of the 1,2,4,5-tetrazine (TTZ) heterocycle (**1**, Fig. 1)), also named *s*-tetrazine, has been increasingly developed in the last two decades, which allowed its use in numerous applications.[1,2] The enhanced electron acceptor properties of tetrazine due to the presence of four sp^2 nitrogen atoms in the ring, providing a low energy π^* type LUMO, make it suitable as synthon in crystal engineering for anion-π interactions[3–7] and strongly facilitate its reduction into stable radical anions.[8–10] Moreover, TTZ derivatives are excellent dienophiles in inverse demand Diels-Alder cycloaddition reactions leading to the formation of 1,2-diazines accompanied by elimination of a nitrogen molecule,[11–15] while when substituted with nitrogen rich units they found use as high energetic materials.[16–18] The substitution scheme is also essential for the luminescence properties of *s*-tetrazines.[2] Indeed, when halogen and/or alkoxy groups are appended to the 3,6 positions of TTZ the corresponding compounds are fluorescent as a result of a symmetry forbidden n-π^* transition arising at 510-530 nm, with a molar extinction coefficient of approx. 1000 L mol^{-1} cm^{-1}.[19–22] Thanks to these different features, it is not surprising that this electron deficient π-aromatic fluorophore has been also involved in π-conjugated materials for organic solar cells[23,24] and as chromophore in switchable fluorescent donor-acceptor systems.[25,26] Finally, as most of the nitrogen containing six-member ring heterocycles, *s*-tetrazine derivatives have attracted interest in coordination chemistry. While the N atoms of tetrazine can in principle act as ligands themselves, the attachment of coordinating groups in positions 3 and 6 affords ligands which can be either chelating, with the participation of tetrazine nitrogen atoms, or ditopic, with the tetrazine ring playing the role of an aromatic bridge. However, the number of available ligands was still rather limited back in 2002 when the previous review on 1,2,4,5-tetrazine based metal complexes was published by Kaim.[27] Since then, the possibilities of functionalization of the tetrazine platform offered by the use of 3,6-dichloro-tetrazine as reactive precursor,[2] and also by the renewal of the interest of the dipyridyl- and dipyrimidyl-tetrazine based complexes in supramolecular chemistry and molecular magnetism, motivated a sustained activity in this area. In this review we discuss the tetrazine based ligands and complexes with an emphasis on the recent examples and a special focus on the solid state structures and physical properties. We have classified the ligands in two families, i.e. symmetric, having the same coordinating groups in the 3,6 positions, and non-symmetric, containing a single coordinating unit (Fig. 1).

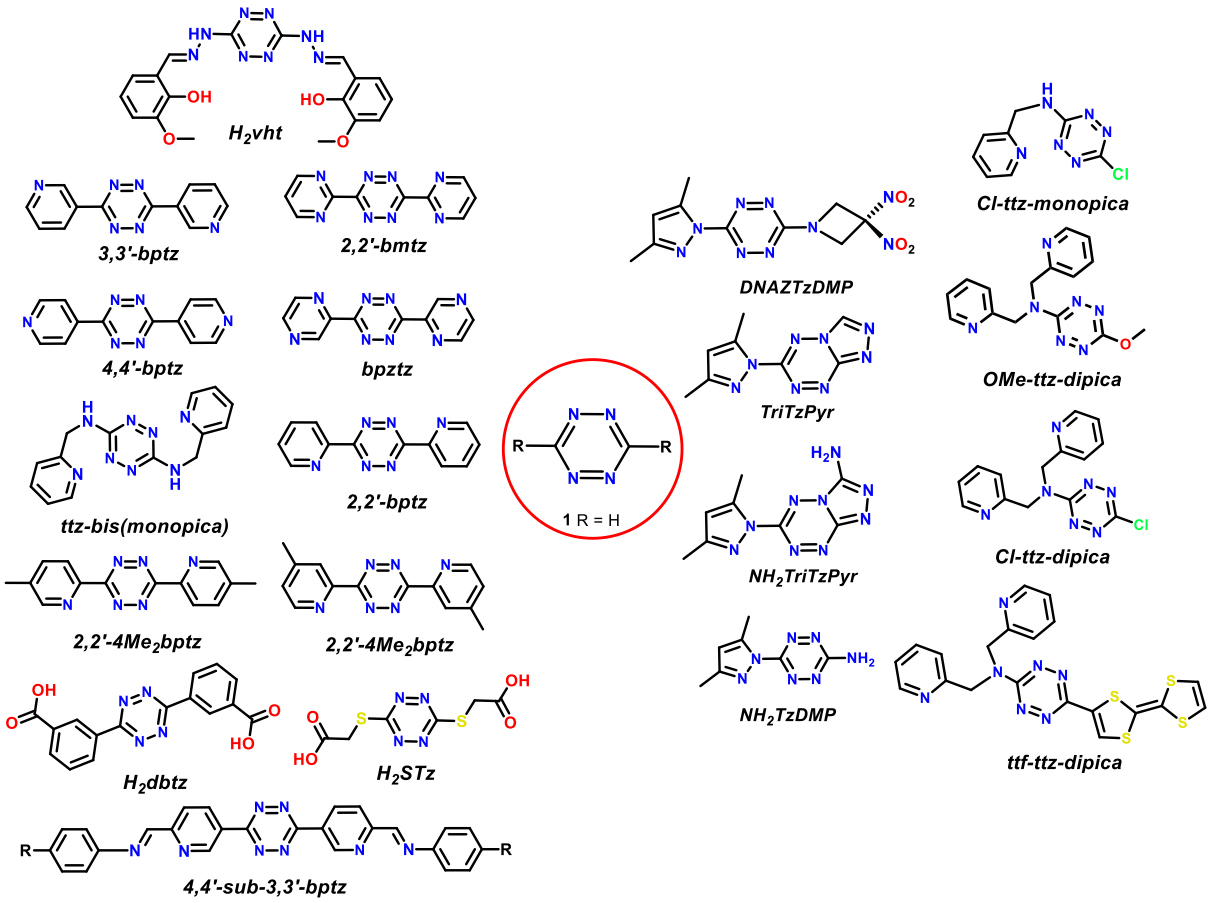

Fig.1 Classification of the *s*-tetrazine based ligands.

The first group of the symmetric ligands includes the ditopic dipyridyl- and dipyrimidyl-tetrazines which are the most employed. The simplicity of their synthesis through Pinner's condensation[2] together with the high yield make these ligands very convenient for coordination towards a large variety of metal centres. However, the coordination chemistry of dipyrimidyl-tetrazines (2,2'-bmtz and bpztz) is comparatively less developed with respect to that of dipyridyl-tetrazines, very likely because of the deactivation of one nitrogen by the second one. Indeed, the pKa of the conjugate acid of pyridine is 5.25, while for pyrimidine it is 1.3.[28]

The second group contains non-symmetric ligands, with two different substituents in positions 3 and 6. An advantage of these molecules is the possibility to limit to one the number of coordinated metal centres per TTZ ligand and to tune the luminescence and electron acceptor properties by the proper choice of the non-coordinating substituent. As mentioned before, the presence of halogen or alkoxy substituents is beneficial for the emissive properties of the TTZ derivative, and thus the modulation of luminescence by coordination can be envisaged. Moreover, additional non-covalent interactions due to the non-coordinating substituent are expected to influence the solid state structures.

2. *s*-1,2,4,5-Tetrazine as ligand

In principle the parent 1,2,4,5-tetrazine **1** itself could act as ligand for metal coordination compounds. However, investigations of basicity of aza-arenes show that tetrazines are very weak bases with values

of $pK_{NH^+} < 0$.[29,30] In addition, the unsubstituted 1,2,4,5-tetrazine is not very stable at room temperature. Therefore, only very few complexes with this ligand have been described.

The first TTZ based complex [Cu(hfac)$_2$(ttz)], reported in 2006 by Li et al.,[31] was prepared by reaction of bis(hexafluoroacetylacetonate)copper(II) with 1,2,4,5-tetrazine in dichloromethane. In the unit cell, there are four non-equivalent Cu(II) ions, the TTZ molecules coordinating the vacant axial position of the metal ion. The bond lengths Cu–N_{ttz} 2.343(3) and 2.466(3) Å are longer than the average Cu–N coordination bonds, meaning that 1,2,4,5-Tetrazine is weakly bounded to the copper ions. This complex starts to decompose at 48 °C with the loss of TTZ.

The other successful attempt towards unsubstituted TTZ complexes was based on the use of the strong donor moiety $[Ru(NH_3)_5]^{2+}$. Indeed, the extremely low-lying π* orbital of TTZ allows an efficient orbital overlap between the metal ions and the ligand. As a result, the dinuclear cationic complex $[\{Ru(NH_3)_5\}_2(\mu\text{-ttz})][BPh_4]_4$ has been isolated.[32] The asymmetric unit contains half the cation as independent motif and the second half is generated by inversion (Fig. 2).

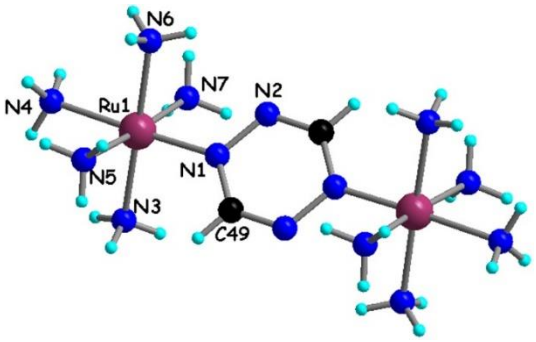

Fig. 2 The crystal structure of the $[\{Ru(NH_3)_5\}_2(\mu\text{-ttz})]^{4+}$ cation.

The longer N1–N2 distances of the TTZ ring in complex compared with the non-coordinated ligand[33] {1.387(5) *vs* 1.334(30) Å} indicate the electron donation from the metal ion to the vacant π* orbitals of TTZ. The presence of coordinated electron-rich $[Ru(NH_3)_5]^{2+}$ metal units influences on the electronic properties of the complex. Thus, two intense transitions in the visible region (750 and 464 nm) were assigned to Ru(II) → TTZ MLCT transitions.

Another interesting family of complexes based on aromatic N-heterocycles was reported by Beckhaus *et al*.[34] The authors described the possibility of the synthesis of titanium based molecular squares and rectangles. This work is very important since the supramolecular chemistry for early transition metals is not that well investigated compared to the late transition metals. [$Cp_2Ti\{\eta^2\text{-}C_2(SiMe_3)_2\}$] and [$(t\text{BuCp})_2Ti\{\eta^2\text{-}C_2(SiMe_3)_2\}$] have been used as source of titanocene fragments, while pyrazine, 4,4'-bipyridine and TTZ served as bridging ligands (Fig. 3 for TTZ).

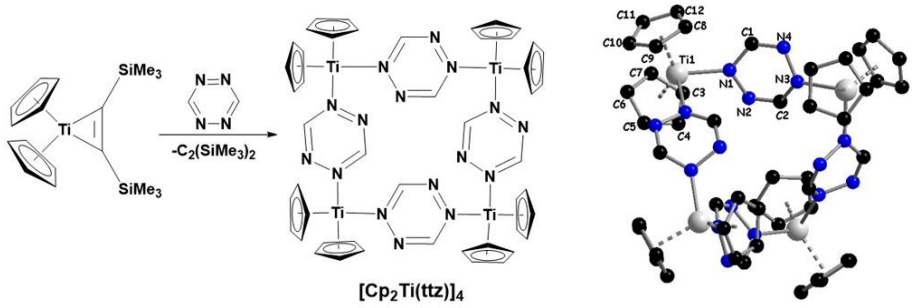

Fig. 3 Synthesis of Ti-based supramolecular complex $[Cp_2Ti(ttz)]_4$ (left) and its crystal structure (right).

Tetrazine coordinates in a bis(monodentate) fashion as observed within the previous examples. Closer analysis of the geometry of complex $[Cp_2Ti(ttz)]_4$ (Fig. 3) indicates that the structure of the compound cannot be considered as molecular square, since the Ti ions do not lie in a single plane but form a tetrahedron. Partial reduction of the ligand also takes place, as demonstrated by the lengthening of the N–N bond in the complex compared with the free TTZ (average values 1.416 Å *vs* 1.321 Å).

Using metal ions such as Ag^+ and Cu^+ with a soft d^{10}-configuration resulted in the family of complexes $[Ag(ttz)(X)]$ (X = NO_3^-, ClO_4^-), $[Ag_2(Me_2ttz)(NO_3)_2]$, $[Ag_2(Me_2ttz)(H_2O)_2(ClO_4)_2]$, $[Ag_3(Me_2ttz)(H_2O)_2(CF_3SO_3)_3]$ and $[Cu_4Cl_4(Me_2ttz)]$, where Me_2ttz is 3,6-dimethyl-1,2,4,5-tetrazine.[35] In these complexes TTZ possesses a unique μ_4-coordination mainly due to the π back-donation of metal ions towards the extremely electron poor TTZ ring. The silver complexes $[Ag(ttz)(X)]$ with nitrate and perchlorate anions are similar (Fig. 4) and can be regarded as 3D coordination polymers. The voids in the frameworks are occupied by the corresponding anions (81% for NO_3^- and 68.9% for ClO_4^-).

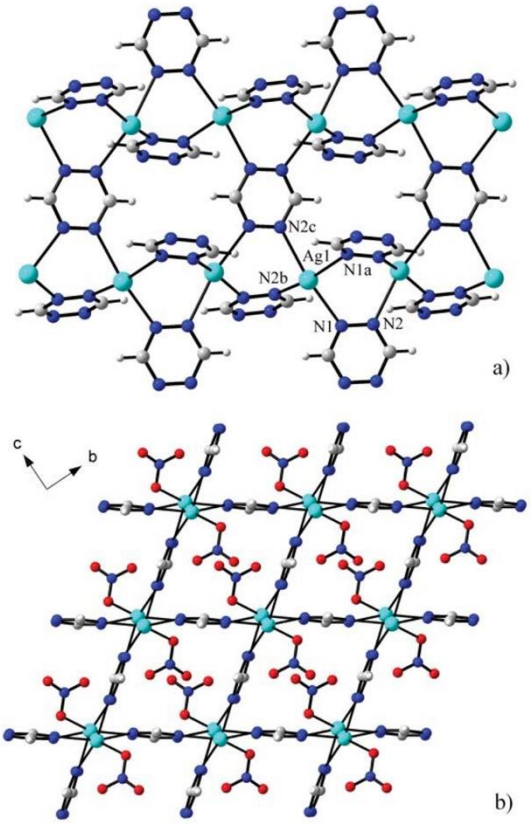

Fig. 4 Metal–organic motif in the structures of [Ag(ttz)(X)] (a); view of the framework in $[Ag(ttz)(NO_3)]$ along the direction of the channels (b). Reproduced from ref. 35 with permission from The Royal Society of Chemistry.

The presence of donating methyl groups in Me_2ttz resulted in the coordination of only two ligands to each metal centre in the crystal structures of $[Ag_2(Me_2ttz)(NO_3)_2]$ and $[Ag_2(Me_2ttz)(H_2O)_2(ClO_4)_2]$. However, the ligands still remain in μ_4-coordination (Fig. 5).

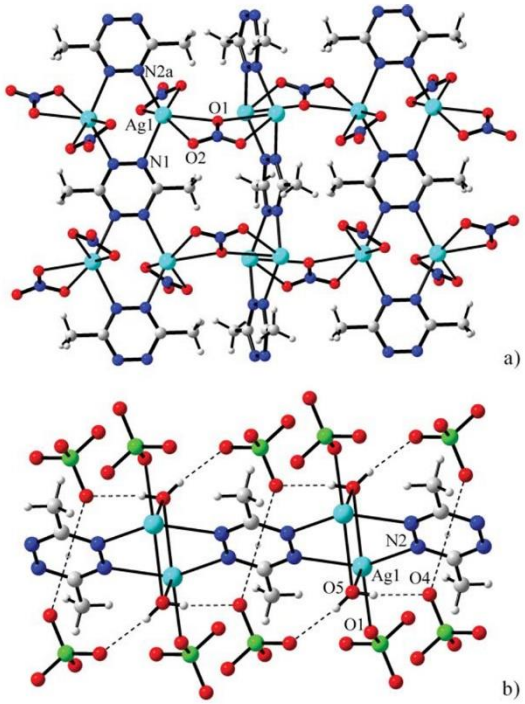

Fig. 5 Fragment of the structure of $[Ag_2(Me_2ttz)(NO_3)_2]$ (a); Similar motif of the structure of $[Ag_2(Me_2ttz)(H_2O)_2(ClO_4)_2]$ with coordinating ClO_4^- anions (b). Reproduced from ref. 35 with permission from The Royal Society of Chemistry.

As mentioned before, the electron-withdrawing character of TTZ ring allows triggers the occurrence of anion-π interactions in the solid state. Thus, each anion (nitrate and perchlorate) form short interactions with the aromatic unit. The values of the O···π contacts for $[Ag_2(Me_2ttz)(NO_3)_2]$ are somewhat longer than the same interactions for $[Ag_2(Me_2ttz)(H_2O)_2(ClO_4)_2]$ (Fig. 6).

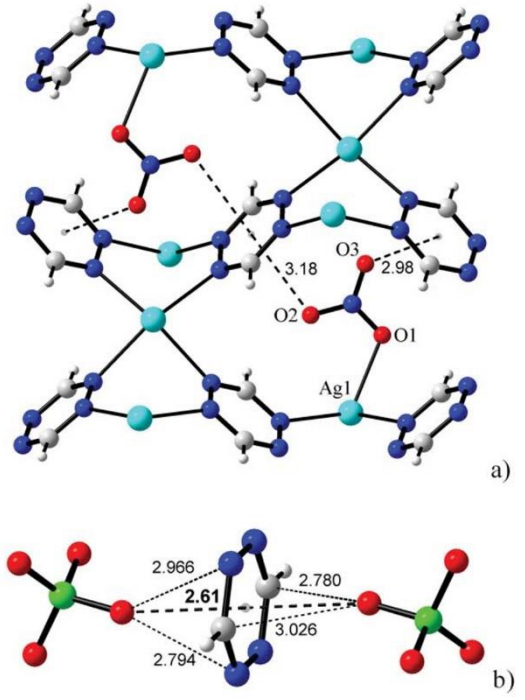

Fig. 6 Anion···π interactions observed in the structures of $[Ag_2(Me_2ttz)(NO_3)_2]$ (a) and $[Ag_2(Me_2ttz)(H_2O)_2(ClO_4)_2]$ (b). Reproduced from ref. 35 with permission from The Royal Society of Chemistry.

The authors explained this feature by the stronger coordination of NO_3^- anion to Ag^+ (Ag-ONO_2 = 2.431 Å *vs* Ag-$OClO_3$ = 2.537 Å). Indeed, the perchlorate anion is not coordinated to the metal ions and, therefore, can form easily stronger π-interaction with the TTZ ring.

Another vivid example of μ_4-coordination of TTZ has been reported in 2018 by Okubo *et al*.[36] They obtained the polymer $[Cu_2Br_2(ttz)]_n$ possessing semiconducting properties. In the solid state structure Cu^+ ion has a tetrahedral coordination geometry formed by two Br anions and two N atoms of the TTZ ring (Fig. 7). The complex shows large absorption band in the near-IR region, indicating a small value of the band gap (E_g). Thus, fitting the Kubelka-Munk plots of $(f(R)\ E)^{1/2}$ *vs* E resulted in the value E_g = 0.71 eV. The direct current electrical resistivity measurements give the estimated conductivity value of $8.17 \cdot 10^{-10}$ S cm^{-1}.

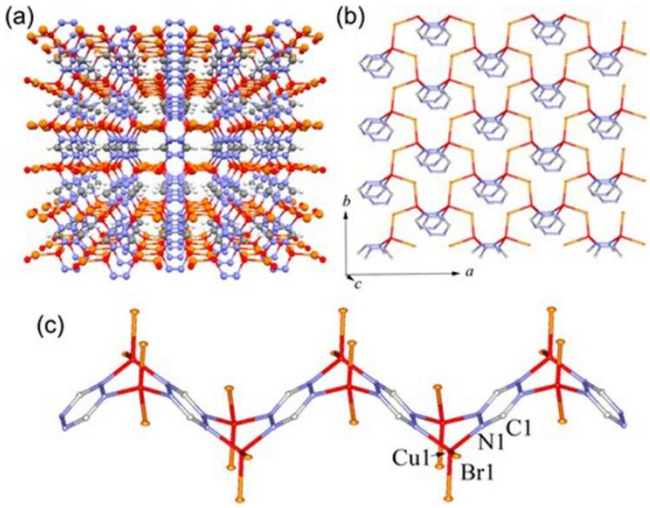

Fig. 7 3D framework of $[Cu_2Br_2(ttz)]_n$ along the *b* axis (a), 2D sheet structure consisting of 1D zigzag Cu^IBr chains along the *b* axis (b), 1D zigzag chain parallel to the *c* axis (c). H atoms are omitted for clarity. Reprinted with permission from ref. 36; Copyright 2018, American Chemical Society.

3. Symmetric ditopic ligands

Due to the multiple chelating modes of these 3,6-disubstituted-1,2,4,5-tetrazine ligands, most of the reported coordination compounds are either discrete polynuclear complexes or extended coordination polymers (CPs). The two only examples of mononuclear complexes are based on 3,6-bis(2-pyridyl)-1,2,4,5-tetrazine (2,2'-bptz) and 3,6-bis(5-methyl-2-pyridine)-1,2,4,5-tetrazine (2,2'-Me_2bptz) (Fig. 1). The position of the nitrogen donor atoms on the pyridyl substituents has a crucial influence on the dimensionality of the resulting coordination compounds. Indeed, most of the discrete polynuclear complexes are based on 2,2'-bptz derivatives, with 50 reported examples, and only 5 examples are based on 4,4'-bptz. On the other hand, 3,3'-bptz only afforded CPs, and a majority of tetrazine-based CPs has been obtained with 4,4'-bptz. In this family of compounds, the dipyridyltetrazine ligand generally acts as a pillar linker which connects 1D or 2D metal-carboxylate networks to afford the 3D porous metal-organic framework (MOF).

3.1. 3,6-bis(2-pyridyl)-1,2,4,5-tetrazine (2,2'-bptz) and methylated derivatives (2,2'-4Me$_2$bptz) and (2,2'-5Me$_2$bptz)

To date, only two examples of mononuclear complexes based on the 3,6-bis(2-pyridyl)-1,2,4,5-tetrazine derivatives have been reported. The first example was a tricarbonylchlororhenium(I) derivative reported by Flood *et al.* in 2010.[37,38] This compound was used as a ligand for the redox-driven supramolecular assembly with Cu(I) and a pseudorotaxane molecule. The second example is a Cd(II) complex of formula [Cd(2,2'-bptz)$_2$I$_2$] reported by Saghatforoush *et al.* in 2016.[39] Interestingly, starting from different cadmium halides, the authors were able to isolate either discrete mononuclear (with CdI_2) and tetranuclear ($CdCl_2$) complexes, or a 1D coordination polymer (with $CdBr_2$). This highlights the versatility of the 2,2'-bptz derivatives to prepare a large variety of coordination compounds with different dimensionalities.

Most of the reported examples of 2,2'-bptz-based coordination compounds are polynuclear complexes, with a majority of them being dinuclear Ru(II), Cu(I)[40–42] or Ag(I)[43–45] complexes. In 1999, Kaim *et al.* reported the first crystal structure of a tetrazine radical anion based complex containing a dinuclear Cu(I) unit of formula {(μ-2,2'-bptz)[Cu(PPh_3)$_2$]$_2$}(BF_4).[46] Four years later, the crystal structure analysis and high-frequency EPR of the related radical complex of formula {(μ-2,2'-bptz)[Cu($AsPh_3$)$_2$]$_2$}(BF_4) confirmed the predominant localization of spin in the tetrazine ring, but revealed a higher spin-orbit coupling constant of As and an increased *g* anisotropy.[47] In the meantime, the delocalized nature of the molecular orbitals in the {(μ-2,2'-bptz)[Ru(bpy)$_2$]$_2$}$^{4+}$ and {(μ-2,2'-bptz)[Cu(PPh_3)$_2$]$_2$}$^{2+}$ radical species were investigated by a resonance Raman study, which was consistent with Class III mixed-valent compounds in the Robin and Day classification.[48] A related Iridium complex was reported by Maekawa *et al.* in 2005.[49] The structural analysis of [Ir$_2$(H)$_4$(PPh_3)$_4$(μ-2,2'-bptz)](PF_6)$_2$·4CH_2Cl_2 revealed the main intramolecular contacts as π–π interactions between the terminal pyridyl rings and the phenyl groups from the PPh_3 ligands. On the contrary, structural analysis of a series of Ag(I)-2,2'-bptz compounds pointed the predominant role of the anion–π interactions over the π–π interactions in the structural motif of the resulting complexes (planar, propeller-like or polymeric structure).[50] In order to better understand the redox processes in 2,2'-bptz-based complexes, some research groups have studied the behaviour of Ru(II) compounds. In 2001, Chellamma and Lieberman have reported the neutral green compound [Ru$_2$(acac)$_4$(μ-2,2'-bptz)], which exhibits a MLCT band at 700 nm, and the delocalized (Class III) mixed-valence blue compound [Ru$_2$(acac)$_4$(2,2'-bptz)](PF_6) which shows an intense MLCT band at 575 nm and a weak band at 1220 nm assigned as an intervalence CT band.[51] The electrochemical properties indicated considerable stabilization of the mixed-valence Ru$_2$(II,III) species. On the other hand, Thomas *et al.* have discussed the Class II/III behaviour of a series of [Ru^{II}([*n*]aneS$_4$)$_2$(μ-2,2'-bptz)](PF_6)$_4$ complexes with the help of spectroelectrochemistry studies (Fig. 8).[52] The observed redox processes were attributed to the [(Ru[12]aneS$_4$)$_2$(μ-2,2'-bptz)]$^{4+/3+}$ reduction couple, which forms a system with two Ru(II) ions bridged by a radical anion 2,2'-bptz$^{\bullet-}$ and suggests that the mixed-valence forms are Class II systems.

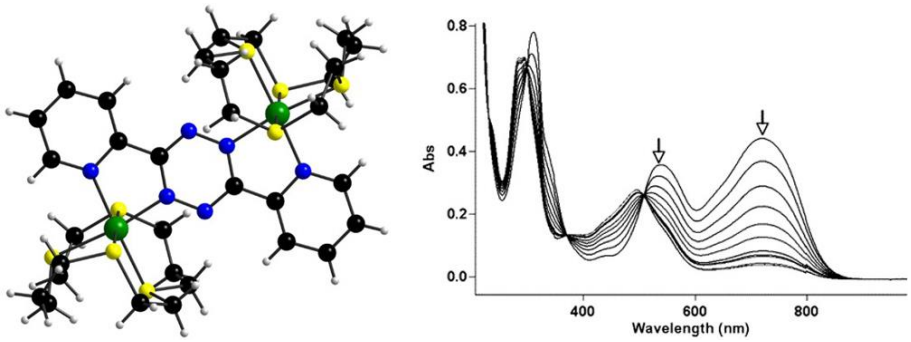

Fig. 8 Structure of the cation (left) and spectroelectrochemistry measurements showing the redox processes occurring at 0.00 V vs Ag/AgCl (right) in the complex $[(Ru[12]aneS_4)_2(\mu\text{-}2,2'\text{-bptz})](PF_6)_4$. Adapted with permission from ref. 52; Copyright 2006, American Chemical Society.

Recently, Fernández *et al.* have reported the anticancer activity against ovarian carcinoma cells of a series of dinuclear Ru(II) complexes of general formula $[\{Ru(bpy)_2\}_2(\mu\text{-L})][CF_3SO_3]_4$ with different bridging ligands L. They have demonstrated that the 2,2'-bptz-based complex $[\{Ru(bipy)_2\}_2(\mu\text{-}2,2'\text{-bptz})][CF_3SO_3]_4$ was the safest considering the compound toxicity.[53]

The only example of a heterodinuclear complex was reported in 2001.[54] The compound $[(\eta^5\text{-}C_5Me_5)ClRh(\mu\text{-}2,2'\text{-bptz})Re(CO)_3Cl](PF_6)$ presents a reversible one-electron uptake followed by a chloride dissociation to produce the neutral Rh(I)-Re(I) compound $[(\eta^5\text{-}C_5Me_5)Rh(\mu\text{-}2,2'\text{-bptz})Re(CO)_3Cl]$. Another strategy was to coordinate the 2,2'-bptz ligand to Ln(III) ions. In 2003, Faulkner, Ward *et al.* reacted 2,2'-bptz with $\{Ln(tta)_3\}$ fragments (Htta = thenoyl(trifluoro)acetone) to afford mononuclear (with Nd and La) or dinuclear complexes (Gd, Yb and Er), yet only the crystal structure of the dinuclear Gd and Yb compounds could be determined. The NIR luminescence of the Yb, Nd and Er complexes were sensitized by the low-energy absorption of 2,2'-bptz transition.[55] Following the same strategy, Dunbar *et al.* have recently reported two Dy(III) compounds, the neutral complex $[Dy(tmhd)_3]_2(2,2'\text{-bptz})$ and its radical form $\{Cp_2Co\}\{[Dy(tmhd)_3]_2(2,2'\text{-bptz})\}$.[56] Both compounds present a slow relaxation of the magnetization below 4 K.

Polynuclear 2,2'-bptz-based complexes of higher nuclearity have also been investigated. In the early 2000s were reported the first two examples of tetranuclear complexes, the paramagnetic Ni(II) compound $[Ni_4(2,2'\text{-bptz})_4(CH_3CN)_8][BF_4]_8\cdot 4CH_3CN$[57] and the Zn(II) compound $[Zn_4(2,2'\text{-bptz})_4(H_2O)_4(CH_3CN)_4](ClO_4)_8\cdot 2CHCl_3\cdot 4CH_3CN$ which was spontaneously resolved as chiral crystals.[58] In 2009, Chen *et al.* have prepared a series of triruthenium-carboxylate complexes and have shown that the low level of π* orbitals of the pyridinyl-tetrazine ligand influences the redox properties since it stabilizes the low-valence Ru_3(III,III,II) and Ru_3(III,II,II) species.[59] Most of the examples of 2,2'-bptz polynuclear compounds were subsequently prepared by the team of Dunbar. The preparation of the pentanuclear complex $[Ni_5(2,2'\text{-bptz})_5(CH_3CN)_{10}][SbF_6]_{10}$ was reported in 2001,[60] and a complete study on a series of Ni(II) and Zn(II) molecular squares and pentagons was undertaken to highlight the template role of the anion on the self-assembly and the nuclearity of these metallacyclophanes.[61] The anion–π interactions were further described as the main driving force in the formation of Fe(II) metallacycles.[62,63] Finally, the same group recently reported the preparation of Co(II) and Ln(III) molecular triangles. The compounds $[Ln_3(hfac)_6(2,2'\text{-bptz}^{\bullet-})_3]$ (Ln = Y or Dy) were obtained after one-electron reduction of the neutral dinuclear complexes $\{[Ln(hfac)_3]_2(2,2'\text{-bptz}^{\bullet-})\}$.[64] Interestingly, during the synthesis of the Co(II) system $[Co_3(2,2'\text{-bptz})_3(dbm)_3]\cdot 2$toluene, the tetranuclear complex $[Co_4(2,2'\text{-bptz})_4(dbm)_4]\cdot 4$MeCN could be obtained by changing the recrystallization solvent of the crude product (Fig. 9).[65] All these resulting polynuclear compounds present strong antiferromagnetic coupling

between metal centres and 2,2'-bptz$^{\bullet-}$ radical bridges. Nevertheless, AC magnetic susceptibility measurements on the trinuclear Ln(III) compounds show the absence of an out-of-phase signal, while the related dinuclear compounds were characterized as SMMs below 15 K with a thermal relaxation barrier of 60 K.

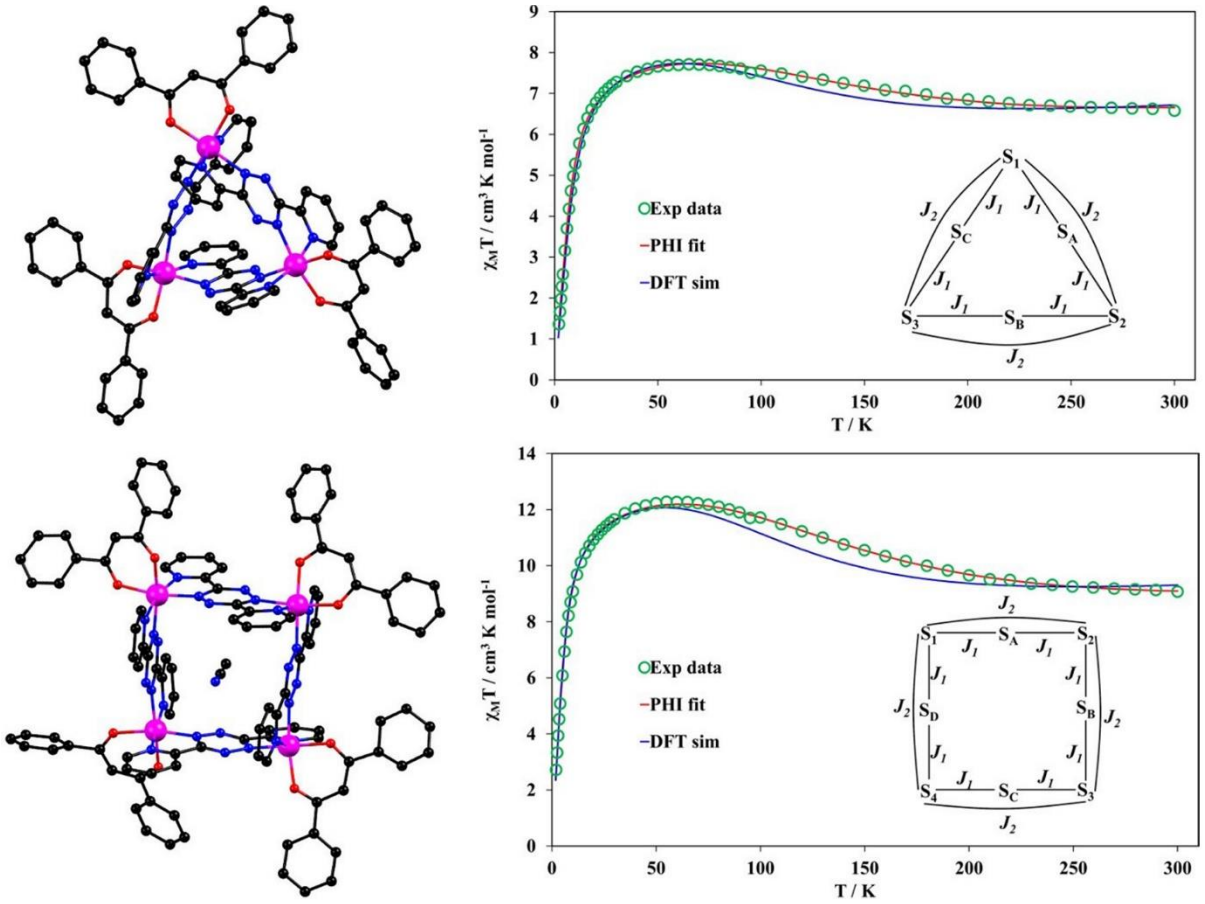

Fig. 9 Structures and temperature dependence of $\chi_M T$ for $[Co_3(2,2'\text{-bptz})_3(dbm)_3]\cdot 2$toluene (top) and $[Co_4(2,2'\text{-bptz})_4(dbm)_4]\cdot 4MeCN$ (bottom). Adapted with permission from ref. 65; Copyright 2017, American Chemical Society.

Finally, the 2,2'-bptz has been used for the preparation of extended coordination polymers. In the early 2000s, the first reported examples consisted on 1D chains with Ag(I)[66] or Cd(II).[67] More interestingly, Xu has reported a 3D heterobimetallic compound of formula $\{[Mn_2Mo(CN)_8(2,2'\text{-bptz})(CH_3CN)_2(H_2O)_2]\cdot 2H_2O\}$ which exhibits a weak antiferromagnetic coupling between Mn(II) ions.[68] More recently, Saghatforoush *et al.* have characterized a series of 1D Hg(II) coordination polymers and calculated their electronic band structure by the DFT method.[69] It indicated a direct band gap in the linear chain polymers $[Hg(2,2'\text{-bptz})Cl_2]$ and $[Hg(2,2'\text{-bptz})Br_2]$, and an indirect semiconductor for the stair-stepped polymer $[Hg_2(2,2'\text{-bptz})(\mu\text{-}I)_2I_2]$. Finally, they have reported in 2018 the formation of 1D-zigzag coordination polymers with Zn(II) and a 2D network with Hg(II).[70] It is worth noting that in this report, the authors have undertaken a CSD structural study on the coordination modes of the 2,2'-bptz ligand.

3.2. 3,6-bis(3-pyridyl)-1,2,4,5-tetrazine (3,3'-bptz)

The coordination of 3,3'-bptz (Fig. 1) has so far resulted in the isolation of extended CPs. The first series has been reported by Schröder *et al.* in 1999.[71] The authors have shown the possibility to tune the dimensionality of the Cd(II) and Zn(II) CPs by the choice of the alcohol solvent. 1D chain structures could thus be obtained in MeOH or EtOH, whereas the use of ^{i}PrOH as solvent resulted in the formation of 2D ladder networks. The same authors have also observed the two possible *cisoid* and *transoid* conformations of 3,3'-bptz in a series of three Ag(I) CPs.[72] In 2005, Aragoni *et al.* have reported a 1D chain structure by coordination of the bis(chelating) ligand to Ni(II).[73] The first example of 3D MOF was reported in 2011.[74] It was based on the combination of $\{Zn_2(COO)_4\}$ clusters with the two organic linkers, i.e. 3,3'-bptz and 4,4'-oxydibenzoic acid, and the structure could be described as a threefold interpenetrated self-catenated network. 3,3'-bptz has been used to link 1D inorganic Co(II) clusters resulting in a 2D structure.[75] In 2015, it was shown that the redox activity of the tetrazine-based ligand was preserved in the CP of formula $[Fe_2NiO(pivalate)_6(3,3'\text{-bptz})_{1.5}]$, with similar redox potentials of the transitions.[76] The same year, the photoluminescence properties of the free ligands 3,3'-bptz and 4,4'-bptz were investigated and compared with the properties of their corresponding Zn(II), Cd(II) and Cu(II) CPs.[77,78] Zhang *et al.* have shown that the emission was blue-shifted in the CPs with respect to the free ligands, accompanied by a fluorescence enhancement which has been attributed to the conformational rigidity of the ligand after coordination to the metal ion (Fig. 10).

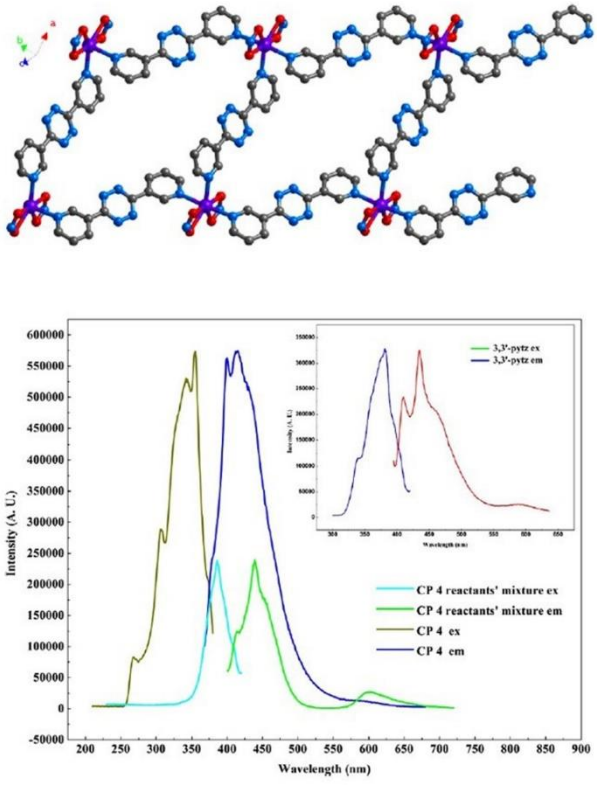

Fig. 10 Structure of the ladder CP $[Cd(\mu_2\text{-}3,3'\text{-bptz})_{1.5}(NO_2)_2]\cdot CH_2Cl_2$ (top) and comparison between the fluorescence properties of the CP and the mixture of the Cd(II) and 3,3'-bptz precursors (bottom). Adapted with permission from ref. 77; Copyright 2015, Elsevier.

Finally, it is worth noting that the team of Nitschke has developed a strategy to obtain polynuclear clusters based on substituted 3,3'-bptz. After condensation of 3,3'-bptz-aldehyde with aniline derivatives, the family of 4,4'-(substituted-methyleneaniline)-3,3'-bptz (Fig. 1) has been used to

prepare tetranuclear Fe^{II} cages. Post-assembly modifications on these cages have revealed the influence of the electron-donating or -withdrawing ability of the aniline substituent on the reactivity of the tetrazine unit.[79]

3.3. 3,6-bis(4-pyridyl)-1,2,4,5-tetrazine (4,4'-bptz)

The 4,4'-bptz (Fig. 1) molecule is by far the most extensively used for the preparation of CPs and MOFs. The first examples were reported in 1997 by the team of Schröder.[80] The authors have reported the series of compounds [Ag(4,4'-bptz)(X)] (X = NO_3^-, BF_4^- and PF_6^-) and already observed the direct influence of the anion on the structure of the CP. The same authors have reported a poly-knotted 3D structure after coordination of 4,4'-bptz with Cd(II) metal ions.[81] 4,4'-bptz has been coordinated to more divalent metal ions, such as Mn(II),[82] Fe(II)[83] and Ni(II),[73] to afford neutral CPs. In the 3D CP [Mn(4,4'-bptz)$(N_3)_2$],[84] it was evidenced the presence of a small antiferromagnetic interaction between Mn(II) metal centres bridged by the 4,4'-bptz unit. In the report of Choe *et al.* in 2009, it was shown that 4,4'-bptz could be coordinated to a paddlewheel Zn building unit, thus acting as a bridge between 2D Zn-porphyrin sheets to afford the 3D compounds [Zn_2(ZnTCPP)(4,4'-bptz)] and [Zn_2(ZnTCPP)(4,4'-bptz)$_{1.5}$] (Fig. 11, TCPP = 5,10,15,20-tetrakis(4-carboxyl)-21*H*,23*H*-porphine).[85] This synthetic strategy has been extensively used in the following, since most of the reported MOFs are heteroleptic pillared layer structures, with the pillar 4,4'-bptz ligand connecting 2D metal-cluster layers. Therefore, in almost all cases, the 4,4'-bptz ligands present the same coordination mode in which the metal ions are only linked to the nitrogen atoms from the pyridyl units. However, after two-electron reduction of the 4,4'-bptz into the 4,5-H_2-4,4'-bptz, Maekawa *et al.* have obtained a Cu(II) CP in which the metal centres could link to one nitrogen atom from the central 4,5-dihydrotetrazine ring to form an unusual 2D architecture.[86] On the other hand, Shi *et al.* have shown that chemical substitution on the tetrazine unit with thiourea was possible and could thus obtained the 3D MOF [Cd(4,4'-bpmtz)], where 4,4'-bpmtz = 1,2-dihydro-1-mercapto-1,2,4,5-tetrazine.[87] More recently, some reports have described the insertion of the 4,4'-bptz linker in a CP by post-synthetic methods. Indeed, the 3D Zn(II) CP [Zn(L)(4,4'-bptz)$_{0.5}$]·3DMF·4H_2O (where L is a terphenyl-tetracarboxylate ligand) was obtained by single-crystal-to-single-crystal (SC-SC) transformation, after dipping crystals of [Zn(L)(3,5-bis(4-pyridyl)triazol-4-amine)$_{0.5}$]·4DMF·8H_2O in a solution of the tetrazine-based ligand.[88] Similarly, postsynthetic modifications of the MOF [Cu_2(mpbatb)] (mpbatb = 4,4',4'',4'''-(1,3-phenylene-bis(azanetriyl))-tetrabenzoate) could afford the compounds [Cu_4(mpbatb)$_2$(4,4'-bptz)$_{0.5}$] and [Cu_4(mpbatb)$_2$(4,4'-bptz)$_{0.5}$(dabco)$_{2.5}$] by successive additions of the ligands 4,4'-bptz and 1,4-diazabicyclo[2.2.2]octane (dabco).[89] Such post-synthetic incorporation of organic linker can modulate the gas-sorption properties of the MOF as highlighted by Suh *et al.* with the compounds [Zn_2(TCPBDA)(4,4'-bptz)]·xDMF·yH_2O (TCPBDA = N,N,N',N'-tetrakis(4-carboxyphenyl)biphenyl-4,4'-diamine).[90]

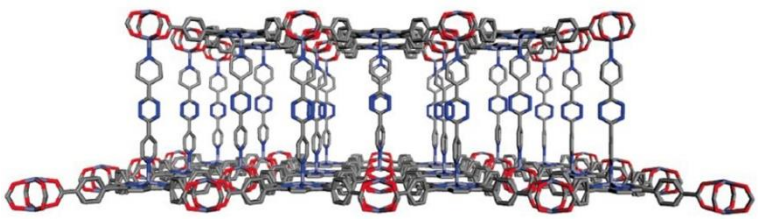

Fig. 11 Structure of the MOF [Zn_2(ZnTCPP)(4,4'-bptz)]. Reprinted with permission from ref. 85; Copyright 2009, American Chemical Society.

In the ten last years, the adsorption properties of 4,4'-bptz-based MOFs have been thoroughly investigated. The microporous MOF $[Zn_2(CNC)_2(4,4'\text{-bptz})]$ (CNC = 4-carboxycinnamic) presents a high H_2 storage density due to the triple framework interpenetration.[91] In the similar 3-fold catenated MOF $[Zn_2(NDC)_2(4,4'\text{-bptz})]$ (NDC = 2,6-naphthalenedicarboxylate), the redox properties of the bridging 4,4'-bptz ligand have been used to modulate the H_2 uptake in the porous material.[92] At the same time, chemical modification of the carboxylate-type ligand could prevent the catenation of the 3D network and thus increase the size of the pores.[93] This strategy allowed different research groups to show the affinity of the 4,4'-bptz-based MOFs toward CO_2 and the selectivity of the adsorption. Indeed, the 2D compound [Zn(3,3',5,5'-tetracarboxydiphenylmethane)(4,4'-bptz)]·DMF·$2H_2O$ presented a maximum CO_2 uptake of 52 $cm^3.g^{-1}$,[94] while the 3D MOF [Cd(4,4'-bpmtz)] revealed an adsorption amount of 79 $cm^3.g^{-1}$,[87] both presenting a very good selectivity for CO_2 over N_2 and H_2. Further studies have demonstrated the impact of the nature of the dinitrogen pillar ligand on the structure and the adsorption efficiency of the resulting MOF.[95] The team of Kitagawa have thus reported a series of 3D Cu(II) and 2D Zn(II) MOFs obtained with pyrazine, dabco, 4,4'-bipyridine, bis(4-pyridyl)benzene, 1,4-bis(4-pyridyl)acetylene and 4,4'-bptz linkers.[96–98] The use of 4,4'-bptz over other dinitrogen ligands usually affords interdigitated frameworks, but still with better affinity for CO_2 adsorption. A similar comparative study was undertaken by Murugavel *et al.* with a series of 3D Zn and Co organophosphates networks and confirmed the high selectivity of the 4,4'-bptz-based compounds (Fig. 12).[99,100] An original type of 1D ladder structure has also been reported by Fletcher *et al.* with the compounds $[Ni(4,4'\text{-bptz})_{1.5}(NO_3)]\cdot n$DCM and $[Co_2(4,4'\text{-bptz})_3(NO_3)_4]\cdot n$DCM.[101] The 1D ladders pack to form a 3D network which shows a reasonable CO_2 uptake. From all these results, tetrazine-based MOFs can be considered as suitable materials for gas separation and selective CO_2 capture.

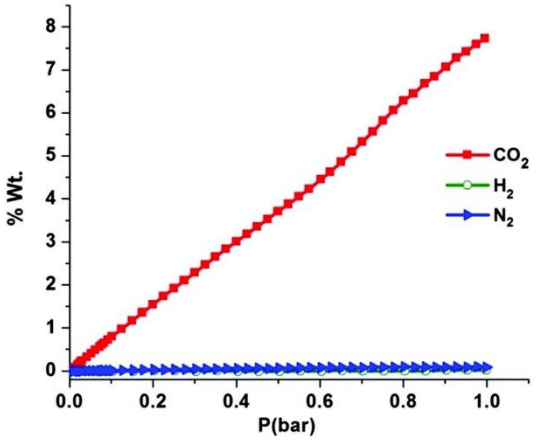

Fig. 12 CO_2, N_2 and H_2 adsorption of the compound $[(Co(dipp)(4,4'\text{-bptz})_{0.5})_4]$ (dipp = 2,6-di-iso-propylphenylphosphate). Reprinted from ref. 100 with permission from The Royal Society of Chemistry.

Moreover, using the 4,4'-bptz as bridging ligand in porous networks has proven to be a good strategy to afford multifunctional materials, for example in the spin-crossover Fe(II) MOF of formula $[Fe(4,4'\text{-bptz})(Au(CN)_2)_2]$ reported by the team of Kepert.[102] Another interesting optical feature of such tetrazine-based MOFs is the solvatochromic behaviour upon incorporating different solvent molecules. For example, the nanotubular MOF $[(WS_4Cu_4)I_2(4,4'\text{-bptz})_3]\cdot$3DMF showed a linear correlation between the optical absorption bands and the polarity of the solvent guest (Fig. 13).[103,104] In the report of Barbour *et al.* this solvatochromism allowed the authors to explain the mechanism of solvent exchange in the 1D CP $[Cu_2(acetate)_2(4,4'\text{-bptz})]\cdot 2CHCl_3$.[105] Finally, one of the most recent interest is to use the chromophore properties of the tetrazine-based ligand to produce hybrid luminescent and photoactive

materials. Therefore, the fluorescence properties of some MOFs constructed from d^{10} metal centres and 4,4'-bptz ligand have been studied.[106] As previously mentioned with 3,3'-bptz-based CPs, a blue-shift in the emission is generally observed after coordination of the 4,4'-bptz to the metal ion in the CP.[74,77] The 4,4'-bptz also contributed to the strong third-order NLO properties of the 3D cluster-based M/S/Cu MOFs reported by Zhang *et al*.[107] Recently, in their study of luminescent Zn(II) and Cd(II) MOFs, Rodríguez-Diéguez *et al.* have shown the first example of blue phosphorescence in the 3D MOF $[Cd_3(\mu_5\text{-btc})_2(\mu\text{-4,4'-bptz})]\cdot 2DMF$, with radiative lifetimes of 0.58-0.76 s and for which the effect could be perceived by the naked eye.[108] Such multifunctional MOFs are of particular interest for the development of smart materials such as photofluorescent sensors.

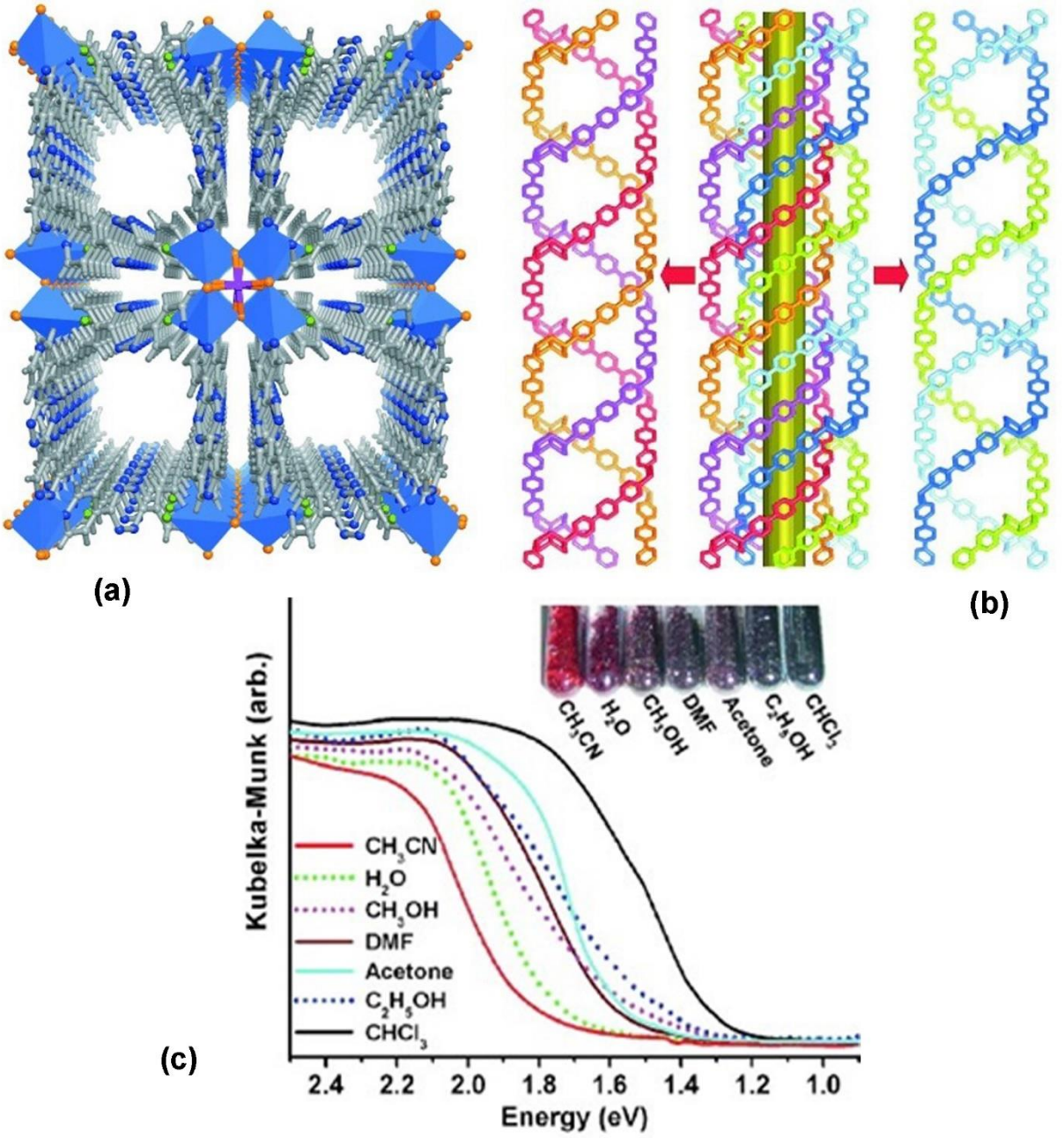

Fig. 13 (a) Structure of $[WS_4Cu_4]I_2(4,4'\text{-bptz})_3]\cdot DMF$. (b) Assembly of six-fold helical chains in the [3+3] arrangement for the formation of the nanotube. (c) UV-Vis spectra and photograph of the solvent inclusion in the MOF. Adapted with permission from ref. 104; Copyright 2012, John Wiley and Sons.

Some examples of discrete polynuclear complexes based on 4,4'-bptz have been also reported. A tetranuclear Re(I) complex has first been described in 2004.[109] In this paper, the authors have demonstrated the ligand-centred mixed valency of the singly reduced molecular rectangles. The second example was reported in 2009 by treatment with $[Cu(dipic)(OH_2)_3]$ giving rise to a binuclear complex.[110] More recently, a series of three Ru(II) metallacycles have been prepared and their anticancer activity demonstrated with the growth inhibition of human colon and gastric cancer cells (Fig. 14).[111] Finally, Hayami *et al.* have reported a spin-crossover binuclear complex in which the 4,4'-bptz bridged two $[Fe(salten)]^+$ moeities.[112] The spin transition was further modified by post-synthesis transformation of the tetrazine unit to its diazine derivative.

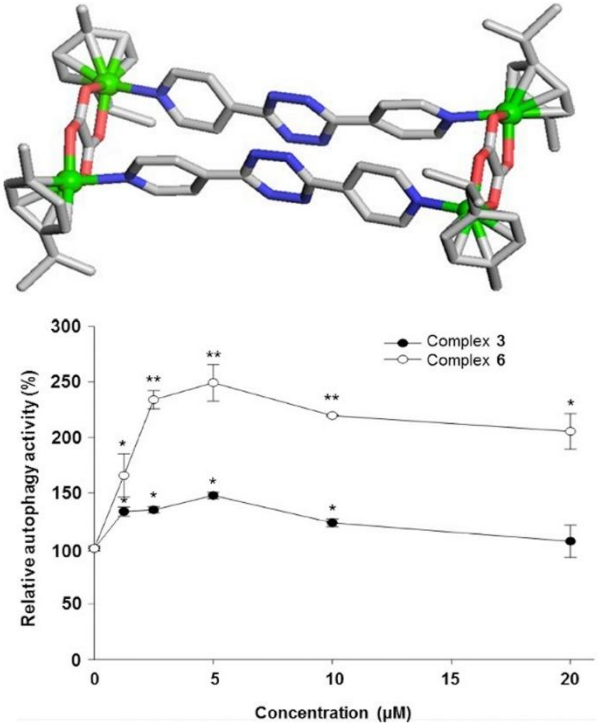

Fig. 14 Structure of the 4,4'-bptz-based Ru(II) metallacycle (top); relative autophagy activity of the compounds studied (bottom). Adapted with permission from ref. 111; Copyright 2015, American Chemical Society.

3.4. 3,6-bis(2-pyrimidyl)-1,2,4,5-tetrazine (2,2'-bmtz)

As related to the 2,2'-bptz ligand, the coordination chemistry of the 2,2'-bmtz molecule (Fig. 1) has been investigated in the two last decades, yet many less examples have been reported. The first crystal structures of 2,2'-bmtz-based complexes were reported by Kaim *et al.* in 2001.[113] In this study, the authors have prepared and characterized the radical complex $[(Cu(PPh_3)_2)_2(2,2'\text{-bmtz})](BF_4)$ and the corresponding 1,4-dihydro species $[(Cu(PPh_3)_2)_2(2,2'\text{-}H_2bmtz)](BF_4)_2$ (2,2'-H_2bmtz = 1,4-dihydro-3,6-bis(2'-pyrimidyl)-1,2,4,5-tetrazine). They have thus observed the pronounced boat conformation of the neutral 2,2'-H_2bmtz, in contrast with the planar structure of the radical anion 2,2'-bmtz after complexation. EPR spectroscopy measurements also revealed the main role of the tetrazine ring in the redox properties of the complexes. The ability of the 2,2'-bmtz ligand to be involved in anion-π interactions for the formation of polynuclear compounds and supramolecular assemblies, as well as the 2,2'-bptz ligand (*vide supra*), have been investigated. Thus, the team of Dunbar have structurally characterized the complex $[\{Fe_5(2,2'\text{-bmtz})_5(CH_3CN)_{10}\}SbF_6][SbF_6]_9$, which was isostructural to the

related 2,2'-bptz-based compound, since the 2,2'-bmtz ligand adopts the *trans*-bis(bidentate) mode.[62] Following these results, the same authors have reported the preparation of dinuclear complexes, such as the SMM of formula $[(Co(TPMA))_2(2,2'\text{-}bmtz^{\bullet-})](CF_3SO_3)_3\cdot CH_3CN$ (TPMA = tris(2-pyridylmethyl)amine) (Fig. 15),[114] and the complex $[(Ni(TPMA))_2(2,2'\text{-}bmtz^{\bullet-})](BF_4)_3$ which exhibits a strong Ni(II)-radical exchange coupling.[115]

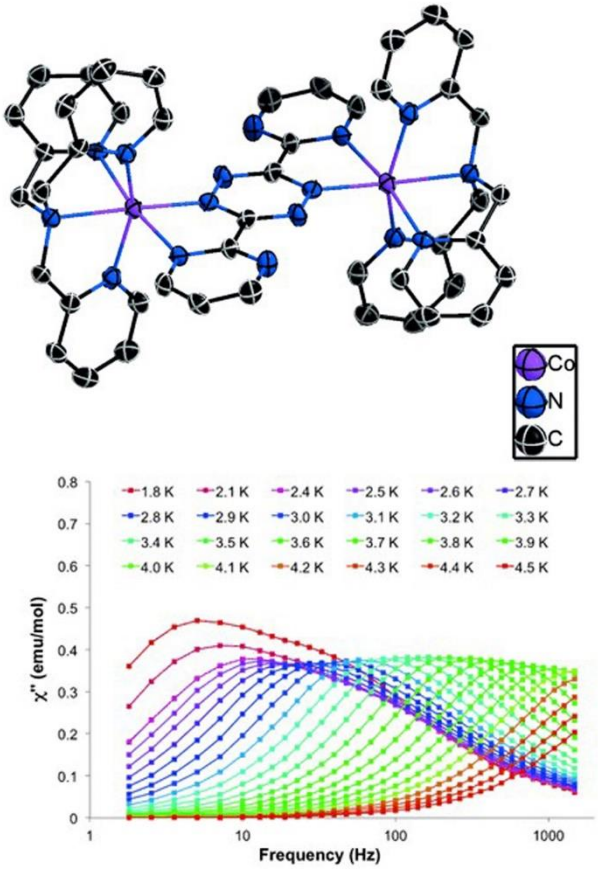

Fig. 15 Structure of the cationic unit in the compound $[(Co(TPMA))_2(2,2'\text{-}bmtz^{\bullet-})](CF_3SO_3)_3\cdot CH_3CN$ (top) and its frequency dependence of χ"in an 800 Oe applied DC field (bottom). Adapted with permission from ref. 114; Copyright 2015, John Wiley and Sons.

Nonetheless, the presence of two extra nitrogen atoms on each pyrimidyl unit offers more coordination possibilities to 2,2'-bmtz compared to 2,2'-bptz. As observed by Murugesu *et al.*, the radical anion 2,2'-$bmtz^{\bullet-}$ could adopt the tetra(bidentate) coordination mode to form the tetranuclear complex $[Ni_4(2,2'\text{-}bmtz^{\bullet-})Cl_6(DMF)_8]Cl\cdot 0.5(H_2O)$ (Fig. 16).[116] In this study, the authors have evidenced the spontaneous reduction of the tetrazine-based ligand upon complexation, without need of air-free conditions or reducing agents, leading to strong ferromagnetic interactions between Ni(II) centres and radical anion bridges.

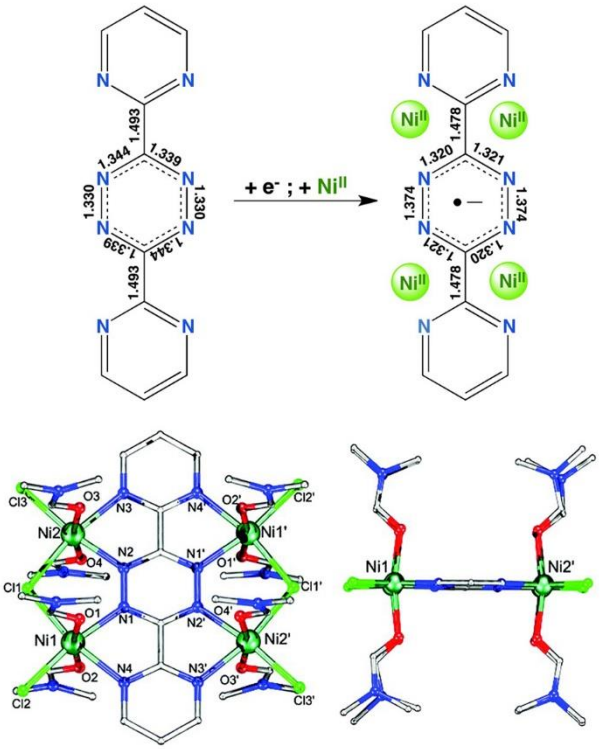

Fig. 16 (a) Coordination mode of the radical anion 2,2'-bmtz$^{\bullet-}$ with selected bond distances in Å. (b) Top and lateral views of the solid state structure of the complex. Reprinted from ref. 116 with permission from The Royal Society of Chemistry.

The two teams of Batten and Murugesu have reported the preparation of 1D and 2D Ag(I) CPs in which the 2,2'-bmtz ligand can adopt the *trans*-bis(bidentate), *cis*-bis(bidentate) or tetra(bidentate) coordination mode.[117,118]

3.5. 3,6-bis(2-pyrazinyl)-1,2,4,5-tetrazine (bpztz)

Since its first synthesis in 2001, only one example of discrete polynuclear complex based on the bpztz ligand (Fig. 1) has been reported. In 2003, Kaim reacted the bpztz ligand to a tricarbonylchlororhenium complex to afford the dinuclear compound [(μ-bpztz){Re(CO)$_3$Cl}$_2$].[119] In this complex, each metal centre was coordinated to one nitrogen atom from the tetrazine ring and the nitrogen atom in position 1 of the pyrazine, therefore the nitrogen atoms in position 4 of each pyrazine remain free. As for the 2,2'-bmtz ligand, the multiple coordination nitrogen atoms makes this ligand more suitable for the preparation of extended networks. This has been demonstrated by the team of Champness, who first reported a series of 1D and 2D Ag(I) coordination polymers with unusual topologies due to the multiple coordination modes of the bpztz ligand, sometimes present among the same network (Fig. 17).[120,121] This feature allowed them to prepare a 1D chain compound with Cd(II) and an unusual 3D coordination polymer with Co(II), in which two independent Co(II) centres present different coordination environments.[122] In spite the promising coordination chemistry with such multimodal ligand, no more examples of coordination complexes or extended networks based on the bpztz ligand have been reported since then.

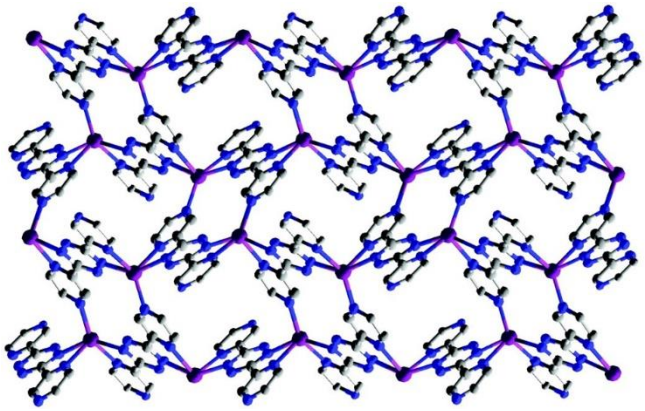

Fig. 17 View of the 2D plane in [Ag(bpztz)]PF_6. Hydrogen atoms and anions are omitted for clarity. Reprinted from ref. 120; copyright 2002 National Academy of Sciences.

3.6. Ttz-bis(monopica) ligand

This ligand has been prepared by the double nucleophilic substitution of 3,6-dichlorotetrazine in 2018 by Avarvari *et al*.[123] The Ttz-bis(monopica) ligand (Fig. 1), similarly to the pyridine and pyrimidine derivative, contains two chelating unit and, moreover, the presence of the amino nitrogen directly linked to the TTZ ring drives the possibility of coordination of this ligand in its anionic form. The Co(II) complex [$Co(hfac)_2$ttz-bis(monopica)]·CH_3CN ($hfac^-$ – hexafluoroacetylacetonate anion) was the first example of coordination compound with this ligand. The attempts to obtain the dinuclear compound in order to investigate the possible Co···Co exchange through the TTZ ring resulted in {[$Co(hfac)_2$-(μ-ttz-bis(monopica))][$Co(hfac)_2(CH_3OH)_2$]}$_n$ complex, which consists of zigzag chains [$Co(hfac)_2$-(μ- ttz-bis(monopica))]$_n$ and guest [$Co(hfac)_2(CH_3OH)_2$] species. Interestingly, only the amino-pyridine moiety participates in the coordination to the Co(II) ions. The direct and alternative current magnetic susceptibility measurements (Fig. 18) suggest that these complexes were new examples of SIMs with octahedral Co(II) ions.

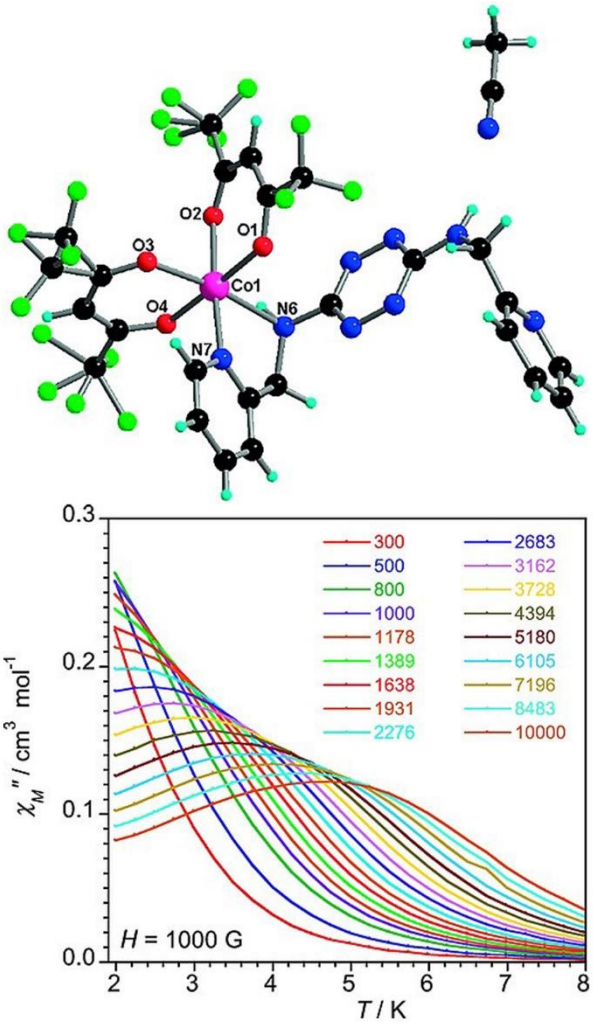

Fig. 18 Crystal structure of [Co(hfac)$_2$ttz-bis(monopica)]·CH_3CN (top) and frequency dependence of the ac out-of-phase molar magnetic susceptibility of [Co(hfac)$_2$ttz-bis(monopica)]·CH_3CN (bottom). Adapted with permission from ref. 123; Copyright 2015, John Wiley and Sons.

3.7. H_2vht ligand

Attempts to combine promising tetrazine rings with the commonly used *o*-vanilin within a polydentate Schiff base ligand were first carried out by Murugesu in 2017.[124] The ligand (Fig. 1) was synthesized from the precursor 3,6-bis(hydrazinyl)-1,2,4,5-tetrazine and *o*-vanilin in methanol solution. Its reaction with Dy(III) and Gd(III) nitrates yielded the $[Dy_4(vht)_4(MeOH)_8](NO_3)_4{\cdot}8.07MeOH{\cdot}0.65H_2O$ and $[Gd_4(vht)_4(MeOH)_8](NO_3)_4{\cdot}8.19MeOH{\cdot}0.91H_2O$ isostructural tetranuclear complexes (Fig. 19).

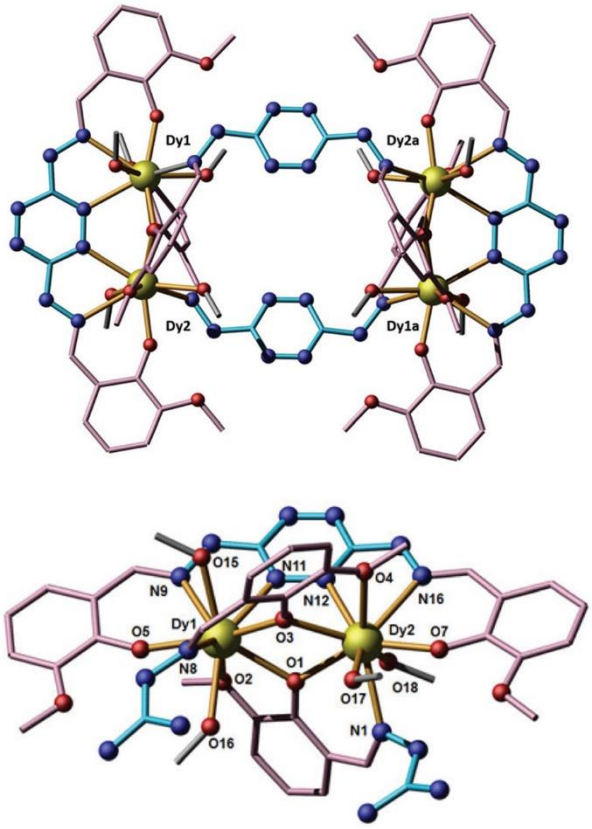

Fig. 19 Crystal structure (top) and dinuclear subunit (bottom) for the Dy complex. Reprinted from ref. 124 with permission from The Royal Society of Chemistry.

These are two complexes composed of two dinuclear subunits, linked by ligand molecules. The metal ions are bridged by the tetrazine ring from the same side, a rare bridging moiety for Ln ions. The magnetic measurements revealed the presence of non-negligible ferromagnetic interaction between the metal centres. Only one *J* parameter was used to modulate the magnetic behaviour of the Dy complex, due to the symmetry equivalence of the dinuclear subunits. The best-fit parameters J = 0.009(3) cm^{-1} and g = 1.982(1) are indicative for weak ferromagnetic interaction. However, the Dy complex displays SMM behaviour, with a barrier U_{eff} = 158 K ($\tau_0 = 1.06 \cdot 10^{-7}$ s).

Performing the synthesis of the Dy complex in ethanol as opposed to methanol and changing the base from NaN_3 to Et_3N leads to the formation of a Dy_8 cluster $[Dy_8(\mu_4\text{-}O)(\mu_3\text{-}OH)_8(vht)_4(NO_3)_2(H_2O)_8](NO_3)_4$.[125] This complex is composed of two distorted $[Dy_4(\mu_3\text{-}OH)_4]^{8+}$ cubanes (Fig. 20)

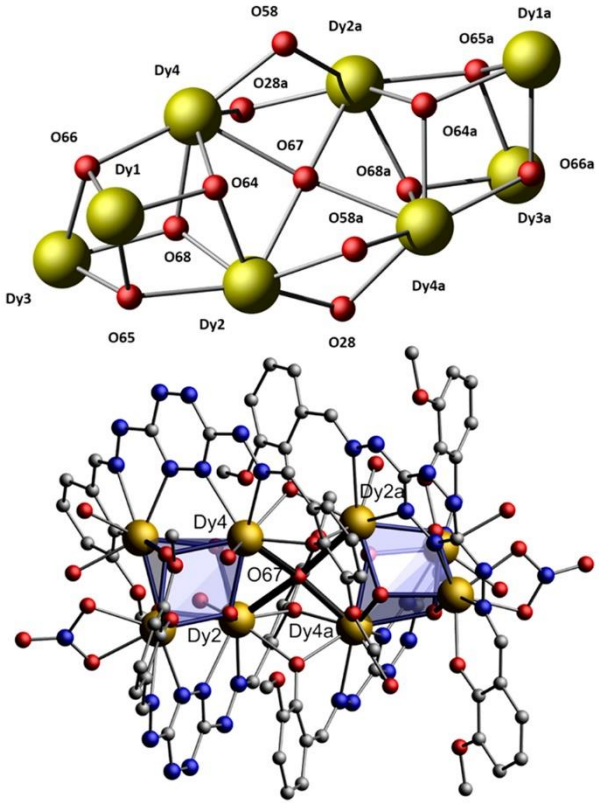

Fig. 20 Polynuclear metallic core (top) and partially labelled crystal structure (bottom) Dy_8 cluster. Reprinted with permission from ref. 125; Copyright 2017, American Chemical Society.

Both cubane moieties are bridged in a unique fashion by a μ_4-O atom. All the H_2vht ligands are fully deprotonated like in the previous complexes, through their phenoxy-groups.

3.8. H_2dbtz and H_2STz ligands

The following ligands contain two carboxylate groups, aimed at using these molecules to construct metal-organic frameworks. The hydrothermal reaction of 3,3'-(1,2,4,5-tetrazine-3,6-diyl)dibenzoic acid (H_2dbtz, Fig. 1) with $Zn(NO_3)_2{\cdot}6H_2O$ and $LaCl_3{\cdot}7H_2O$ resulted in $[Zn(dbtz)(H_2O)]_n$ and $\{[La_2(dbtz)_3(H_2O)_2](H_2O)_6\}_n$ coordination polymers.[126] The X-ray analysis revealed a two-dimensional network for the Zn complex, stabilized by coordinated water molecules. However, the crystal structure of the La complex consists of a three-dimensional framework with channels occupied by water molecules. Investigation of the optical properties in the solid state showed that the emission of both complexes is more intense than that of the pure H_2dbtz ligand. Thus, the spectra of Zn and La compounds exhibit broad emission bands centred at 454 and 461 nm, respectively, upon excitation at 310 nm.

Later on, in 2017, the synthesis and characterization of a Zr(IV) MOF with a *s*-tetrazine dicarboxylic acid (H_2STz) were reported by Devic *et al*.[127] The complex, formulated $Zr_6O_8(STz)_4(solvent)_n$, is able to detect electron-rich molecules due to the quenching of its fluorescence, centred on the TTZ ligand.

4. Non-symmetric monotopic ligands

As was already mentioned, the presence of different substituents plays a key role in the modulation of the physical properties of ttz-based compounds. In the pioneering work of our group,[128] the electron deficient tetrazine ring has been covalently linked to the known electron donor tetrathiafulvalene (TTF)[129] unit affording the donor-acceptor molecule **2** (Fig. 21). Its deep photophysical study combined with DFT calculations show the presence of low energy $\pi_{TTF} \rightarrow \pi^*_{ttz}$ intramolecular charge transfer.

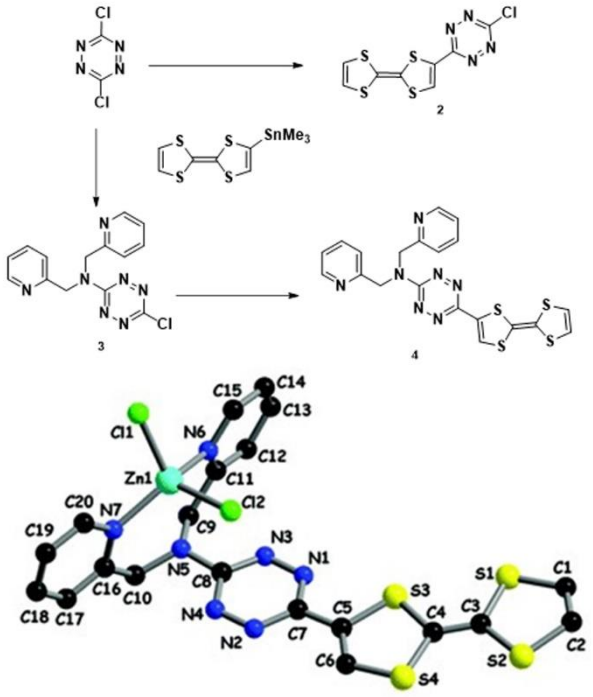

Fig. 21 Synthesis of TTF-TTZ-Cl **2** and TTF-TTZ-dipica **4** (top) and crystal structure of [$ZnCl_2$(TTF-TTZ-dipica)] with the atom labelling scheme (bottom). Adapted from ref. 128 with permission from The Royal Society of Chemistry.

The precursor **2** was used to prepare the multifunctional ligand TTF-TTZ-dipica **4**. However, the yield of the direct coupling reaction was low, therefore another way for its synthesis was elaborated. Accordingly, compound **3** was synthesized first, then further cross-coupling gave the desired TTF-TTZ-dipica **4.** As a preliminary test of coordination, the zinc complex [$ZnCl_2$(**4**)] has been obtained (Fig. 21). The structure shows Cl···TTZ anion-π interactions, with the corresponding distance of 3.24 Å.

The precursor **3**, namely Cl-ttz-dipica also was found to be a perspective platform for the synthesis of compounds possessing tunable photophysical or magnetic properties.[130] A series of binuclear neutral complexes [Cl-ttz-dipica-MCl_2]$_2$ (M – Mn^{II}, Co^{II}, Zn^{II} and Cd^{II}) has been obtained and their properties were examined. The coordination of diamagnetic zinc(II) and cadmium (II) ions leads to the switch-on of the luminescence. The Cl-ttz-dipica ligand emits very weakly with the value of quantum yields less than 0.01 %, while the coordination of the metal ions leads to relatively strong emission in the visible region (570 nm). The reason of the higher quantum yield for Zn and Cd complexes results from the involvement of the amino N atom in coordination (N2, Fig. 22a) thus hampering the conjugation with the ttz ring.

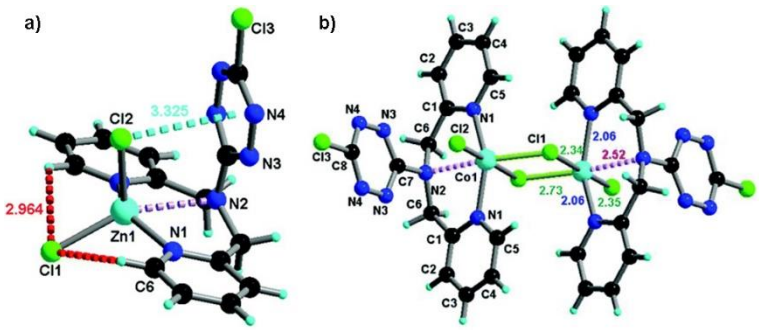

Fig. 22 Molecular structures of $[Cl\text{-ttz-dipica-}ZnCl_2]_2$ (a) and $[(Cl\text{-ttz-dipica})CoCl_2]_2$ (b) together with the atom numbering scheme and Co–X (Cl, N) distances. Adapted from ref. 130 with permission from The Royal Society of Chemistry.

In the case of complexes with paramagnetic Mn^{II} and Co^{II} ions an antiferromagnetic interaction takes place in the dimanganese(II) compound (J = -1.25 cm^{-1}), while in the corresponding binuclear $[Cl\text{-ttz-dipica-}CoCl_2]_2$ complex (Fig. 22b) the metal centres are ferromagnetically coupled (J = +0.55 cm^{-1}).

Very recently the possibility of exchanging Cl-substituent in Cl-ttz-dipica with OMe-group has been demonstrated.[131] The reaction has been performed in methanol solution of Cl-ttz-dipica and sodium methoxide, affording the new ligand OMe-ttz-dipica **5** (Fig. 23).

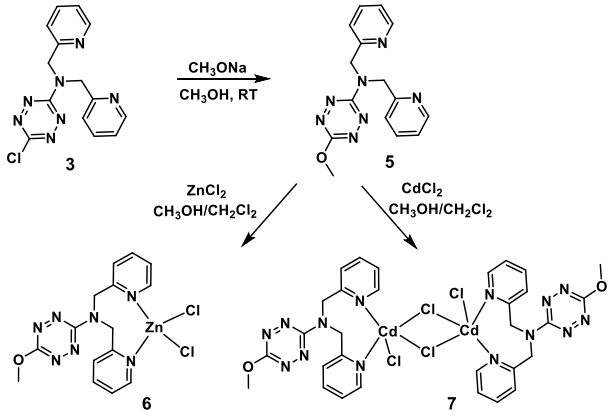

Fig. 23 Synthesis of the OMe-ttz-dipica ligand **5** and its Zn and Cd complexes **6** and **7**. Adapted with permission from ref. 131; Copyright 2019, Elsevier.

While the ligand **5** is not emissive, the coordination of diamagnetic Zn^{II} and Cd^{II} metal ions switch-on the luminescence of the tetrazine moiety. The emission behaviour of these complexes is similar to those with the Cl-ttz-dipica ligand **3**, but in the present case the maximum of the emission is slightly red shifted.

In most of the ligands we have discussed so far the tetrazine ring could in principle be reduced to radical anion. However, the electron-poor character of tetrazine unit has never been used to enhance the acidity of the amino substituents towards anionic ligands. A recent work of our group has been devoted to the incorporation of one amino-picolyl group on the tetrazine ring, resulting in the new Cl-ttz-monopica ligand.[132] By changing the experimental conditions a series of mono- and binuclear Cu complexes has been obtained. Of particular interest are the binuclear mixed valence $Cu^{1.5}Cu^{1.5}$ complexes $[Cu_2(\mu\text{-Cl})(Cl\text{-ttz-monopica})_2]$ and $[Cu_2(\mu\text{-triflate})(Cl\text{-ttz-monopica})_2]$ (Fig. 24).

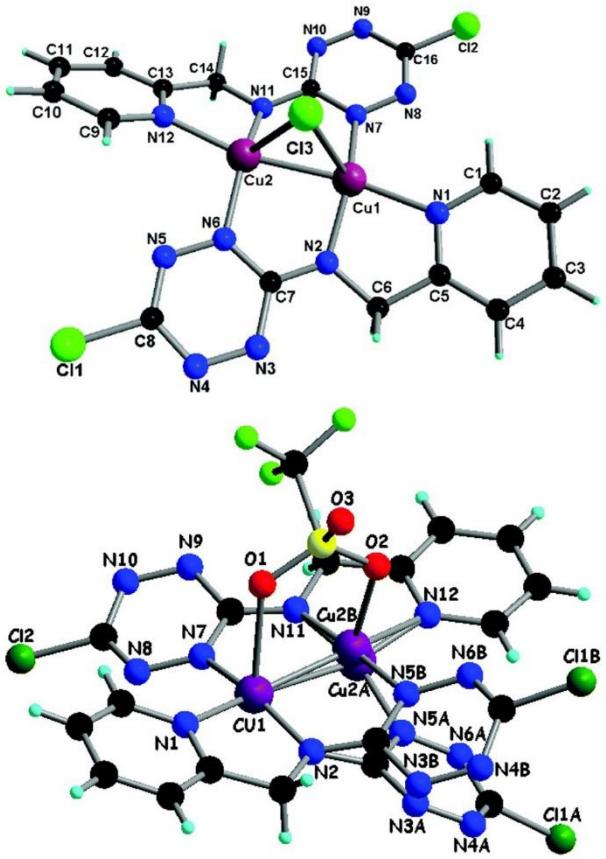

Fig. 24 Molecular structures of [Cu_2(μ-Cl)(Cl-ttz-monopica)$_2$] (top) and [Cu_2(μ-triflate)(Cl-ttz-monopica)$_2$] (bottom) together with the atom numbering scheme. Adapted from ref. 132 with permission from The Royal Society of Chemistry.

Both complexes possess similar structural features. Thus, the Cu ions are tetracoordinated – the equatorial positions for both complexes are occupied by three nitrogen atoms from the tetrazine ligand, while the axial coordination sites are occupied by the bridging anions (Cl^- and $triflate^-$). It should be noted that the ligand is deprotonated and coordinates in its anionic form, being the equivalent of a guanidinate. But the most important feature is the close Cu···Cu distances (2.4314(4) Å for [Cu_2(μ-Cl)(Cl-ttz-monopica)$_2$] and 2.5413(4) Å for [Cu_2(μ-triflate)(Cl-ttz-monopica)$_2$]). Evidence for the mixed-valence nature of these complexes has been provided by EPR spectroscopy. The EPR spectra, measured at different temperature, are characteristic and show seven lines hyperfine coupling (Fig. 25a). Simulation of the spectrum (Fig. 25 b) resulted in the following parameters g_x = 2.050 ± 0.005, g_y = 2.120 ± 0.005, and g_z = 2.158 ± 0.002, with the corresponding hyperfine coupling constants of A_x = 30 ± 5 MHz, A_y = 222 ± 3 MHz, and A_z = 420 ± 5 MHz. Accordingly, these complexes can be considered as a III class mixed-valence where the single electron is delocalized between the two metal centres. The magnetic data and DFT calculations support this suggestion.

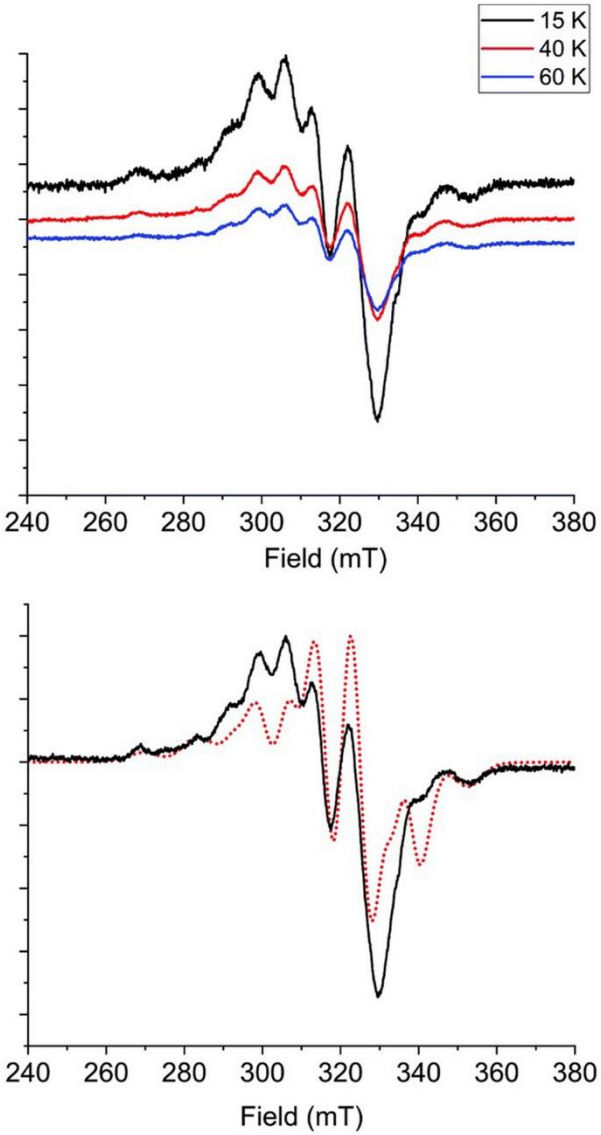

Fig. 25 The EPR spectra of $[Cu_2(\mu\text{-}Cl)(Cl\text{-}ttz\text{-}monopica)_2]$ (top) and comparison between experimental (continuous black line) and simulated (dotted red line) spectrum at 60 K (bottom). Adapted from ref. 132 with permission from The Royal Society of Chemistry.

The energetic tetrazine-pyrazole based ligands (NH_2TzDMP and DNAZTzDMP, Fig. 1) have been used to obtain series of first row transitional metal complexes, displaying rich electrochemical and photophysical properties.[133] Thus, complexes $[(NH_2TzDMP)_3Fe](X)_2$ and $[(DNAZTzDMP)_3Fe](X)_2$, where X = BF_4^-, NO_3^-, have been isolated through the reaction of the ligand with the $Fe^{II}(H_2O)_6(BF_4)_2$ and $Fe(NO_3)_3$ precursors. The tetrazine based ligand stabilizes the Fe(II) oxidation state. Both complexes are octahedral and contain 3 molecules of the ligand in a *mer* arrangement. The ability of the ligand to stabilize unusual oxidation states has been further investigated by its reaction with copper precursors. Thus, reaction of the above mentioned ligands with $Cu(NO_3)_2$ yielded the five coordinated $[(NH_2TzDMP)_2Cu(NO_3)][NO_3]$ and $[(DNAZTzDMP)_2Cu(NO_3)][NO_3]$, while the $Cu^I(CH_3CN)_4(PF_6)$ compound afforded the tetrahedral $[(NH_2TzDMP)_2Cu][PF_6]$, $[(DNAZTzDMP)_2Cu][PF_6]$ complexes. The electrochemical measurements of the Fe complexes show three reduction waves from -0.40 to -1.24 V *vs* Fc, corresponding to the reduction of each of the three NH_2TzDMP ligands to radical anion. The

presence of the fourth oxidation wave at 1.18-1.33 V corresponds to the Fe^{II}/Fe^{III} couple. All the copper complexes exhibit similar trends. Thus, the oxidation waves from 0.25 to 0.41 V were assigned to the Cu^{I}/Cu^{II} couple. However, in case of the copper compounds only one reduction process has been observed at -0.6 V and was attributed to the reduction of the tetrazine ligands. Although both ligands have similar electronic and electrochemical properties, their explosive behaviour is very different. Thus, the oxygen balance of all DNAZTzDMP containing complexes varies from -70 to -83 %, which is close to the one in TNT (trinitrotoluene). All these compounds possess thermal stability similar to PETN (Pentaerythritol tetranitrate) and they are sensitive toward impact detonation.

This work was further developed by Myers with examples of Fe(II) complexes with the N-containing TriTzPyr and NH_2TriTzPyr ligands. Interestingly, the explosion of the compounds $[(TriTzPyr)_3Fe](ClO_4)_2$ and $[(NH_2TriTzPyr)_3Fe](ClO_4)_2$ was found to be initiated with near-infrared lasers.[134]

5. Conclusions and outlook

The coordination chemistry of *s*-tetrazine has afforded numerous examples of functional coordination polymers, molecular boxes and discrete SMMs/SIMs. Indeed, the dipyridyl- and dipyrimidyl-tetrazine ligands offer a variety of coordination modes (that can be anticipated by the position of the N atom in the pyridyl/pyrimidyl units) and therefore a variety of coordination compounds with different dimensionalities. On the other hand, the recent development of non-symmetric di-substituted tetrazines has opened a new perspective for the design of (multi)functional materials, for example by the insertion of TTF derivatives. Other recent examples are the versatile amino-substituted tetrazine ligands, in which the amino group can be deprotonated due to the electron-withdrawing effect of the tetrazine unit, thus making them suitable for the preparation of coordination compounds with controlled nuclearity and crystal structures. More chemical design on the *s*-tetrazine is expected to bring, besides new functionalities, a possible control over the electrochemical and photophysical properties of the resulting material. Indeed, if the coordination chemistry of the *s*-tetrazine-based ligands is well established, it remains a challenge to play with its electronic and optical properties in order to modulate the properties of the complex and thus produce smart materials. The reduction of the tetrazine unit into stable radical anions represents a step in this direction. Another valuable perspective consists in the preparation of chiral tetrazine-based ligands and complexes, which remain unexplored to date as it has been shown that the combination of chirality with conducting, magnetic or optical properties can result in synergistic effects.[135]

Conflicts of interest

There are no conflicts to declare.

Acknowledgements

This work was supported by the CNRS, the University of Angers, the French Embassy in Kiev (grant to O.S.) and by the National Agency for Research (ANR, Project 15-CE29-0006-01 ChiraMolCo).

ORCID

Oleh Stetsiuk: 0000-0003-3269-7466

Alexandre Abhervé: 0000-0002-3883-310X

Narcis Avarvari: 0000-0001-9970-4494

Notes and references

1 N. Saracoglu, *Tetrahedron*, 2007, **63**, 4199–4236.

2 G. Clavier and P. Audebert, *Chem. Rev.*, 2010, **110**, 3299–3314.

3 H. T. Chifotides and K. R. Dunbar, *Acc. Chem. Res.,* 2013, **46**, 894–906.

4 M. Savastano, C. Bazzicalupi, C. Giorgi, C. García-Gallarín, M. D. López de la Torre, F. Pichierri, A. Bianchi and M. Melguizo, *Inorg. Chem.,* 2016, **55**, 8013–8024.

5 M. Savastano, C. Bazzicalupi, C. García, C. Gellini, M. D. López de la Torre, P. Mariani, F. Pichierri, A. Bianchi and M. Melguizo, *Dalton Trans.,* 2017, **46**, 4518–4529.

6 M.-Y. Zhao, D.-X. Wang and M.-X. Wang, *J. Org. Chem.*, 2018, **83**, 1502–1509.

7 M. Savastano, C. García-Gallarín, M. D. López de la Torre, C. Bazzicalupi, A. Bianchi, M. Melguizo, *Coord. Chem. Rev.*, 2019, **397**, 112–137.

8 B. J. Jordan, M. A. Pollier, L. A. Miller, C. Tiernan, G. Clavier, P. Audebert and V. M. Rotello, *Org. Lett.*, 2007, **9**, 2835–2838.

9 Q. Zhou, P. Audebert, G. Clavier, R. Méallet-Renault, F. Miomandre, Z. Shaukat, T.-T. Vu and J. Tang, *J. Phys. Chem. C*, 2011, **115**, 21899–21906.

10 E. Kurach, D. Djurado, J. Rimarčik, A. Kornet, M. Wlostowski, V. Lukeš, J. Pécaut, M. Zagorska and A. Pron, *Phys. Chem. Chem. Phys.*, 2011, **13**, 2690–2700.

11 M. D. Helm, A. Plant and J. P. A. Harrity, *Org. Biomol. Chem.*, 2006, **4**, 4278–4280.

12 A.-C. Knall and C. Slugovc, *Chem. Soc. Rev.*, 2013, **42**, 5131–5142.

13 F. Liu, Y. Liang and K. N. Houk, *J. Am. Chem. Soc.*, 2014, **136**, 11483–11493.

14 O. Roling, A. Mardyukov, S. Lamping, B. Vonhören, S. Rinnen, H. F. Arlinghaus, A. Studera and B. J. Ravoo, *Org. Biomol. Chem.*, 2014, **12**, 7828–7835.

15 D. Wang, W. Chen, Y. Zheng, C. Dai, K. Wang, B. Ke and B. Wang, *Org. Biomol. Chem.*, 2014, **12**, 3950–3955.

16 M. H. V. Huynh, M. A. Hiskey, D. E. Chavez, D. L. Naud and R. D. Gilardi, *J. Am. Chem. Soc.*, 2005, **127**, 12537–12543.

17 D. E. Chavez, S. K. Hanson, J. M. Veauthier and D. A. Parrish, *Angew. Chem. Int. Ed.*, 2013, **52**, 6876–6879.

18 C. J. Snyder, D. E. Chavez, G. H. Imler, E. F. C. Byrd, P. W. Leonard and D. A. Parrish, *Chem. Eur. J.,* 2017, **23**, 16466–16471.

19 P. Audebert, F. Miomandre, G. Clavier, M.-C. Vernières, S. Badré and R. Méallet-Renault, *Chem. Eur. J.*, 2005, **11**, 5667–5673.

20 Y.-H. Gong, F. Miomandre, R. Méallet-Renault, S. Badré, L. Galmiche, J. Tang, P. Audebert and G. Clavier, *Eur. J. Org. Chem.*, 2009, 6121–6128.

21 C. Quinton, V. Alain-Rizzo, C. Dumas-Verdes, G. Clavier, F. Miomandre and P. Audebert, *Eur. J. Org. Chem.*, 2012, 1394–1403.

22 C. Quinton, V. Alain-Rizzo, C. Dumas-Verdes, F. Miomandre and P. Audebert, *Electrochim. Acta*, 2013, **110**, 693–701.

23 Z. Li, J. F. Ding, N. Song, J. Lu and Y. Tao, *J. Am. Chem. Soc.*, 2010, **132**, 13160–13161.

[24] Z. Li, J. F. Ding, N. Song, X. M. Du, J. Y. Zhou, J. P. Lu and Y. Tao, *Chem. Mater.*, 2011, **23**, 1977–1984.

[25] C. Quinton, S.-H. Chi, C. Dumas-Verdes, P. Audebert, G. Clavier, J. W. Perry and V. Alain-Rizzo, *J. Mater. Chem. C,* 2015, **3**, 8351–8357.

[26] C. Quinton, V. Alain-Rizzo, C. Dumas-Verdes, G. Clavier, L. Vignau and P. Audebert, *New J. Chem.,* 2015, **39**, 9700–9713.

[27] W. Kaim, *Coord. Chem. Rev.*, 2002, **230**, 126–139.

[28] J. A. Joule and K. Mills, The Diazines: Pyridazine, Pyrimidine, and Pyrazine: Reactions and Synthesis. In *Heterocyclic Chemistry*, 5th Edition ed.; Wiley-Blackwell, 2003.

[29] W. Kaim and S. Kohlmann, *Inorg. Chem.,* 1987**, 26**, 68–77.

[30] J. Spanget-Larsen, *J. Chem. Soc., Perkin Trans. 2,* 1985, 417–419.

[31] L. Li, C. P. Landee, M. M. Turnbull and B. Twamley, *J. Coord. Chem.,* 2006**, 59**, 1311–1320.

[32] S. Tampucci, M. Belicchi Ferrari, L. Calucci, G. Pelosi and G. Denti, *Inorg. Chim. Acta,* 2007**, 360**, 2814–2818.

[33] R. E. Smalley, L. Wharton, D. H. Levy and D. W. Chandler, *J. Mol. Spectrosc.,* 1977**, 66**, 375–388.

[34] S. Kraft, E. Hanuschek, R. Beckhaus, D. Haase and W. Saak, *Chem. Eur. J.,* 2005**, 11**, 969–978.

[35] I. y. A. Gural'skiy, D. Escudero, A. Frontera, P. V. Solntsev, E. B. Rusanov, A. N. Chernega, H. Krautscheid and K. V. Domasevitch, *Dalton Trans.,* 2009, 2856–2864.

[36] T. Okubo, K. Himoto, K. Tanishima, S. Fukuda, Y. Noda, M. Nakayama, K. Sugimoto, M. Maekawa and T. Kuroda-Sowa, *Inorg. Chem.,* 2018**, 57**, 2373–2376.

[37] G. Li, K. Parimal, S. Vyas, C. M. Hadad, A. H. Flood and K. D. Glusac, *J. Am. Chem. Soc.*, 2009, **131**, 11656–11657.

[38] K. Parimal, E. H. Witlicki and A. H. Flood, *Angew. Chem. Int. Ed.*, 2010, **49**, 4628–4632.

[39] L. Saghatforoush, Z. Khoshtarkib, H. Keypour and M. Hakimi, *Polyhedron*, 2016, **119**, 160–174.

[40] W.-Y. Yeh, G.-H. Lee and S.-M. Peng, *Inorg. Chim. Acta*, 2006, **359**, 659–664.

[41] M. Maekawa, T. Miyazaki, K. Sugimoto, T. Okubo, T. Kuroda-Sowa, M. Munakata and S. Kitagawa, *Dalton Trans.*, 2013, **42**, 4258–4266.

[42] M. Maekawa, K. Sugimoto, T. Okubo, T. Kuroda-Sowa and M. Munakata, *Inorg. Chim. Acta*, 2017, **467**, 204–211.

[43] E. C. Constable, C. E. Housecroft, B. M. Kariuki, N. Kelly and C. B. Smith, *Inorg. Chem. Commun.*, 2002, **5**, 199–202.

[44] B. L. Schottel, J. Bacsa and K. R. Dunbar, *Chem. Commun.*, 2005, 46–47.

[45] E. C. Constable, C. E. Housecroft, M. Neuburger, S. Reymann and S. Schaffner, *CrystEngComm*, 2008, **10**, 991–995.

[46] M. Schwach, H.-D. Hausen and W. Kaim, *Inorg. Chem.*, 1999, **38***,* 2242–2243.

[47] S. Ye, W. Kaim, B. Sarkar, B. Schwederski, F. Lissner, T. Schleid, C. Duboc-Toia and J. Fiedler, *Inorg. Chem. Commun.*, 2003, **6**, 1196–1200.

[48] K. C. Gordon, A. K. Burrell, T. J. Simpson, S. E. Page, G. Kelso, M. I. J. Polson and A. Flood, *Eur. J. Inorg. Chem.*, 2002, 554–563.

[49] M. Maekawa, H. Konaka, T. Minematsu, T. Kuroda-Sowa, Y. Suenaga and M. Munakata, *Inorg. Chim. Acta*, 2005, **358**, 1317–1321.

[50] B. L. Schottel, H. T. Chifotides, M. Shatruk, A. Chouai, L. M. Pérez, J. Bacsa and K. R. Dunbar, *J. Am. Chem. Soc.*, 2006, **128**, 5895–5912.

[51] S. Chellamma and M. Lieberman, *Inorg. Chem.*, 2001, **40**, 3177–3180.

[52] M. Newell, J. D. Ingram, T. L. Easun, S. J. Vickers, H. Adams, M. D. Ward and J. A. Thomas, *Inorg. Chem.*, 2006, **45**, 821–827.

[53] O. A. Lenis-Rojas, C. Roma-Rodrigues, A. R. Fernandes, F. Marques, D. Pérez-Fernández, J. Guerra-Varela, L. Sánchez, D. Vázquez-García, M. López-Torres, A. Fernández and J. J. Fernández, *Inorg. Chem.*, 2017, **56**, 7127–7144.

[54] T. Scheiring, J. Fiedler and W. Kaim, *Organometallics*, 2001, **20**, 1437–1441.

[55] N. M. Shavaleev, S. J. A. Pope, Z. R. Bell, S. Faulkner and M. D. Ward, *Dalton Trans.*, 2003, 808–814.

[56] B. S. Dolinar, S. Gómez-Coca, D. I. Alexandropoulos and K. R. Dunbar, *Chem. Commun.*, 2017, **53**, 2283–2286.

[57] C. S. Campos-Fernández, R. Clérac and K. R. Dunbar, *Angew. Chem. Int. Ed.*, 1999, **38**, 3477–3479.

[58] X.-H. Bu, H. Morishita, K. Tanaka, K. Biradha, S. Furusho and M. Shionoya, *Chem. Commun.*, 2000, 971–972.

[59] F.-R. Dai, H.-Y. Ye, B. Li, L.-Y. Zhang and Z.-N. Chen, *Dalton Trans.*, 2009, 8696–8703.

[60] C. S. Campos-Fernández, R. Clérac, J. M. Koomen, D. H. Russell and K. R. Dunbar, *J. Am. Chem. Soc.*, 2001, **123**, 773–774.

[61] C. S. Campos-Fernández, B. L. Schottel, H. T. Chifotides, J. K. Bera, J. Bacsa, J. M. Koomen, D. H. Russell and K. R. Dunbar, *J. Am. Chem. Soc.*, 2005, **127**, 12909–12923.

[62] I. D. Giles, H. T. Chifotides, M. Shatruk and K. R. Dunbar, *Chem. Commun.*, 2011, **47**, 12604–12606.

[63] H. T. Chifotides, I. D. Giles and K. R. Dunbar, *J. Am. Chem. Soc.*, 2013, **135**, 3039–3055.

[64] B. S. Dolinar, D. I. Alexandropoulos, K. R. Vignesh, T. James and K. R. Dunbar, *J. Am. Chem. Soc.*, 2018, **140**, 908–911.

[65] D. I. Alexandropoulos, B. S. Dolinar, K. R. Vignesh and K. R. Dunbar, *J. Am. Chem. Soc.*, 2017, **139**, 11040–11043.

[66] E. C. Constable, C. E. Housecroft, B. M. Kariuki, N. Kelly and C. B. Smith, *C. R. Chimie 5*, 2002, 425–430.

[67] M. Du, X.-H. Bu, K. Biradha and M. Shionoya, *J. Chem. Res.*, 2002, **5**, 247–249.

[68] X.-J. Xu, *Acta Crystallogr.*, 2014, **C70**, 1029–1032.

[69] L. Saghatforoush, Z. Khoshtarkib, V. Amani, A. Bakhtiari, M. Hakimi and H. Keypour, *J. Solid State Chem.*, 2016, **233**, 311–319.

[70] L. Saghatforoush, K. Moeini, V. Golsanamlou, V. Amani, A. Bakhtiari and Z. Mardani, *Inorg. Chim. Acta*, 2018, **483**, 392–401.

[71] M. A. Withersby, A. J. Blake, N. R. Champness, P. A. Cooke, P. Hubberstey, W.-S. Li and M. Schröder, *Inorg. Chem.*, 1999, **38**, 2259–2266.

[72] M. A. Withersby, A. J. Blake, N. R. Champness, P. A. Cooke, P. Hubberstey, W.-S. Li and M. Schröder, *Cryst. Eng.*, 1999, **2**, 123–136.

[73] M. C. Aragoni, M. Arca, N. R. Champness, M. De Pasquale, F. A. Devillanova, F. Isaia, V. Lippolis, N. S. Oxtoby and C. Wilson, *CrystEngComm*, 2005, **7**, 363–369.

[74] J. Li, Y. Peng, H. Liang, Y. Yu, B. Xin, G. Li, Z. Shi and S. Feng, *Eur. J. Inorg. Chem.*, 2011, 2712–2719.

[75] T. Zheng, S.-S. Bao, M. Ren and L.-M. Zheng, *Dalton Trans.*, 2013, **42**, 16396–16402.

[76] A. S. Lytvynenko, R. A. Polunin, M. A. Kiskin, A. M. Mishura, V. E. Titov, S. V. Kolotilov, V. M. Novotortsev and I. L. Eremenko, *Theor. Exp. Chem.*, 2015, **51**, 54–61.

[77] H. Zhao, D. Jia, J. Li, G. J. Moxey and C. Zhang, *Inorg. Chim. Acta*, 2015, **432**, 1–12.

[78] J. Li and C. Zhang, *J. Chem. Sci.*, 2015, **127**, 1871–1882.

[79] D. A. Roberts, B. S. Pilgrim, J. D. Cooper, T. K. Ronson, S. Zarra and J. R. Nitschke, *J. Am. Chem. Soc.*, 2015, **137**, 10068–10071.

[80] M. A. Withersby, A. J. Blake, N. R. Champness, P. Hubberstey, W.-S. Li and M. Schröder, *Angew. Chem. Int. Ed.*, 1997, **36**, 2327–2329.

[81] M. A. Withersby, A. J. Blake, N. R. Champness, P. A. Cooke, P. Hubberstey and M. Schröder, *J. Am. Chem. Soc.*, 2000, **122**, 4044–4046.

[82] P. Seth, A. Bauzá, A. Frontera, C. Massera, P. Gamez and A. Gosh, *CrystEngComm*, 2013, **15**, 3031–3039.

[83] M. A. D. Roxburgh, S. Zaiter, X. I. B. Hudson, B. R. Mullaney, J. E. Clements, B. Moubaraki, K. S. Murray, S. M. Neville and C. J. Kepert, *Aust. J. Chem.*, 2017, **70**, 623–631.

[84] P. Kar, M. G. B. Drew, C. J. Gómez-García and A. Gosh, *Inorg. Chem.*, 2013, **52**, 1640–1649.

[85] H. Chung, P. M. Barron, R. W. Novotny, H.-T. Son, C. Hu and W. Choe, *Cryst. Growth Des.*, 2009, **9**, 3327–3332.

[86] M. Maekawa, K. Sugimoto, T. Okubo, T. Kuroda-Sowa and M. Munakata, *Inorg. Chim. Acta*, 2015, **426**, 64–70.

[87] K. Liu, X. Han, Y. Zou, Y. Peng, G. Li, Z. Shi and S. Feng, *Inorg. Chem. Commun.*, 2014, **39**, 131–134.

[88] T. K. Pal, S. Neogi and P. K. Bharadwaj, *Chem. Eur. J.*, 2015, **21**, 16083–16090.

[89] P. Müller, F. M. Wisser, V. Bon, R. Grünker, I. Senkovska and S. Kaskel, *Chem. Mater.*, 2015, **27**, 2460–2467.

[90] H. J. Park, Y. E. Cheon and M. P. Suh, *Chem. Eur. J.*, 2010, **16**, 11662–11669.

[91] M. Xue, S. Ma, Z. Jin, R. M. Schaffino, G.-S. Zhu, E. B. Lobkovsky, S.-L. Qiu and B. Chen, *Inorg. Chem.*, 2008, **47**, 6825–6828.

[92] K. L. Mulfort, T. M. Wilson, M. R. Wasielewski and J. T. Hupp, *Langmuir*, 2009, **25**, 503–508.

[93] O. K. Farha, C. D. Malliakas, M. G. Kanatzidis and J. T. Hupp, *J. Am. Chem. Soc.*, 2010, **132**, 950–952.

[94] S. Sen, S. Neogi, A. Aijaz, Q. Xu and P. K. Bharadwaj, *Dalton Trans.*, 2014, **43**, 6100–6107.

[95] L.-W. Lee, T.-T. Luo, S.-H. Lo, G.-H. Lee, S.-M. Peng, Y.-H. Liu, S.-L. Lee and K.-L. Lu, *CrystEngComm*, 2015, **17**, 6320–6327.

[96] R. Matsuda, T. Tsujino, H. Sato, Y. Kubota, K. Morishige, M. Takata and S. Kitagawa, *Chem. Sci.*, 2010, **1**, 315–321.

[97] Y. Hijikata, S. Horike, M. Sugimoto, H. Sato, R. Matsuda and S. Kitagawa, *Chem. Eur. J.*, 2011, **17**, 5138–5144.

[98] Y. Hijikata, S. Horike, M. Sugimoto, M. Inukai, T. Fukushima and S. Kitagawa, *Inorg. Chem.*, 2013, **52**, 3634–3642.

[99] A. Ch. Kalita, N. Gogoi, R. Jangir, S. Kuppuswamy, M. G. Walawalkar and R. Murugavel, *Inorg. Chem.*, 2014, **53**, 8959–8969.

[100] S. K. Gupta, S. Kuppuswamy, J. P. S. Walsh, E. J. L. McInnes and R. Murugavel, *Dalton Trans.*, 2015, **44**, 5587–5601.

[101] E. Dooris, C. A. McAnally, E. J. Cussen, A. R. Kennedy and A. J. Fletcher, *Crystals*, 2016, **6**, 14.

[102] J. E. Clements, J. R. Price, S. M. Neville and C. J. Kepert, *Angew. Chem. Int. Ed.*, 2014, **53**, 10164–10168.

[103] Z.-Z. Lu, R. Zhang, Y.-Z. Li, Z.-J. Guo and H.-G. Zheng, *J. Am. Chem. Soc.*, 2011, **133**, 4172–4174.

[104] Z.-Z. Lu, R. Zhang, Z.-R. Pan, Y.-Z. Li, Z.-J. Guo and H.-G. Zheng, *Chem. Eur. J.*, 2012, **18**, 2812–2824.

[105] C. X. Bezuidenhout, C. Esterhuysen and L. J. Barbour, *Chem. Commun.*, 2017, **53**, 5618–5621.

[106] B. Fernández, J. M. Seco, J. Cepeda, A. J. Calahorro and A. Rodríguez-Diéguez, *CrystEngComm*, 2015, **17**, 7636–7645.

[107] J. Li, D. Jia, S. Meng, J. Zhang, M. P. Cifuentes, M. G. Humphrey and C. Zhang, *Chem. Eur. J.*, 2015, **21**, 7914–7926.

[108] J. M. Seco, S. Pérez-Yáñez, D. Briones, J. A. García, J. Cepeda and A. Rodríguez-Diéguez, *Cryst. Growth Des.*, 2017, **17**, 3893–3906.

[109] P. H. Dinolfo, M. E. Williams, C. L. Stern and J. T. Hupp, *J. Am. Chem. Soc.*, 2004, **126**, 12989–13001.

[110] M. Felloni, A. J. Blake, P. Hubberstey, C. Wilson and M. Schröder, *Cryst. Growth Des.*, 2009, **9**, 4685–4699.

[111] A. Dubey, Y. J. Jeong, J. H. Jo, S. Woo, D. H. Kim, H. Kim, S. C. Kang, P. J. Stang and K.-W. Chi, *Organometallics*, 2015, **34**, 4507–4514.

[112] Y. Komatsumaru, M. Nakaya, F. Kobayashi, R. Ohtani, M. Nakamura, L. F. Lindoy and S. Hayami, *Z. Anorg. Allg. Chem.*, 2018, **644**, 729–734.

[113] M. Glöckle, K. Hübler, H.-J. Kümmerer, G. Denninger and W. Kaim, *Inorg. Chem.*, 2001, **40**, 2263–2269.

[114] T. J. Woods, M. F. Ballesteros-Rivas, S. M. Ostrovsky, A. V. Palii, O. S. Reu, S. I. Klokishner and K. R. Dunbar, *Chem. Eur. J.*, 2015, **21**, 10302–10305.

[115] T. J. Woods, H. D. Stout, B. S. Dolinar, K. R. Vignesh, M. F. Ballesteros-Rivas, C. Achim and K. R. Dunbar, *Inorg. Chem.*, 2017, **56**, 12094–12097.

[116] M. A. Lemes, G. Brunet, A. Pialat, L. Ungur, I. Korobkov and M. Murugesu, *Chem. Commun.*, 2017, **53**, 8660–8663.

[117] K. Chainok, S. M. Neville, C. M. Forsyth, W. J. Gee, K. S. Murray and S. R. Batten, *CrystEngComm*, 2012, **14**, 3717–3726.

[118] D. A. Safin, A. Pialat, A. A. Leitch, N. A. Tumanov, I. Korobkov, Y. Filinchuk, J. L. Brusso and M. Murugesu, *Chem. Commun.*, 2015, **51**, 9547–9550.

[119] B. Sarkar, W. Kaim, T. Schleid, I. Hartenbach and J. Fiedler, *Z. Anorg. Allg. Chem.*, 2003, **629**, 1353–1357.

[120] N. S. Oxtoby, A. J. Blake, N. R. Champness and C. Wilson, *Proc. Natl. Acad. Sci. USA*, 2002, **99**, 4905–4910.

[121] N. S. Oxtoby, A. J. Blake, N. R. Champness and C. Wilson, *Dalton Trans.*, 2003, 3838–3839.

[122] N. S. Oxtoby, N. R. Champness and C. Wilson, *CrystEngComm*, 2005, **7**, 284–288.

[123] O. Stetsiuk, A. El-Ghayoury, F. Lloret, M. Julve and N. Avarvari, *Eur. J. Inorg. Chem.,* 2018**,** 449–457.

[124] T. Lacelle, G. Brunet, A. Pialat, R. J. Holmberg, Y. Lan, B. Gabidullin, I. Korobkov, W. Wernsdorfer and M. Murugesu, *Dalton Trans.*, 2017, **46**, 2471–2478.

[125] T. Lacelle, G. Brunet, R. J. Holmberg, B. Gabidullin and M. Murugesu, *Cryst. Growth Des.*, 2017, **17**, 5044–5048.

[126] A. J. Calahorro, A. Peñas-Sanjuan, M. Melguizo, D. Fairen-Jimenez, G. Zaragoza, B. Fernández, A. Salinas-Castillo and A. Rodríguez-Diéguez, *Inorg. Chem.*, 2013, **52**, 546–548.

[127] P. Rouschmeyer, N. Guillou, C. Serre, G. Clavier, C. Martineau, P. Audebert, E. Elkaïm, C. Allain and T. Devic, *Inorg. Chem.*, 2017, **56**, 8423–8429.

[128] F. Pop, J. Ding, L. M. L. Daku, A. Hauser and N. Avarvari, *RSC Advances,* 2013**, 3**, 3218–3221.

[129] F. Pop and N. Avarvari, *Chem. Commun.*, 2016, **52**, 7906–7927.

[130] I. Nazarenko, F. Pop, Q. Sun, A. Hauser, F. Lloret, M. Julve, A. El-Ghayoury and N. Avarvari, *Dalton Trans.,* 2015**, 44**, 8855–8866.

[131] O. Stetsiuk, A. El-Ghayoury, A. Hauser and N. Avarvari, *Polyhedron,* 2019**, 170**, 232–238.

[132] O. Stetsiuk, S. R. Petrusenko, L. Sorace, A. Lupan, A. A. A. Attia, V. N. Kokozay, A. El-Ghayoury and N. Avarvari, *Dalton Trans.,* 2019**, 48**, 11966–11977.

[133] T. W. Myers, D. E. Chavez, S. K. Hanson, R. J. Scharff, B. L. Scott, J. M. Veauthier and R. Wu, *Inorg. Chem.,* 2015**, 54**, 8077–8086.

[134] T. W. Myers, J. A. Bjorgaard, K. E. Brown, D. E. Chavez, S. K. Hanson, R. J. Scharff, S. Tretiak and J. M. Veauthier, *J. Am. Chem. Soc.,* 2016**, 138**, 4685–4692.

[135] F. Pop, N. Zigon and N. Avarvari, *Chem. Rev.* **2019**, *119*, 8435–8478.

Table of Contents Entry

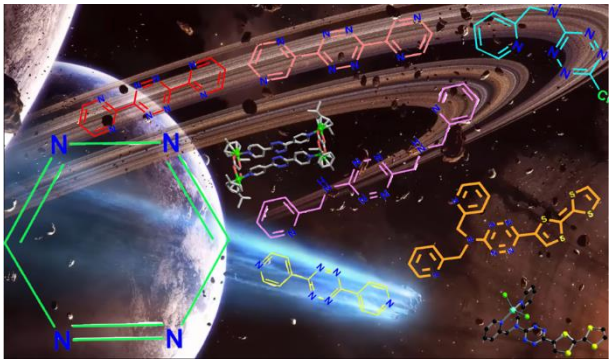

The 1,2,4,5-tetrazine based ligands and complexes are reviewed with a special focus on their crystalline structure and physical properties.